NIH Public Access
Author Manuscript
Sci Total Environ. Author manuscript; available in PMC 2016 February 01.

Published in final edited form as:
Sci Total Environ. 2015 February 1; 505: 1291–1307. doi:10.1016/j.scitotenv.2014.04.089.

Flow and sorption controls of groundwater arsenic in individual boreholes from bedrock aquifers in central Maine, USA

Qiang Yang[1,2], **Charles W. Culbertson**[3], **Martha G. Nielsen**[3], **Charles W. Schalk**[3], **Carole D. Johnson**[4], **Robert G. Marvinney**[5], **Martin Stute**[1], and **Yan Zheng**[1,2]

[1]Lamont-Doherty Earth Observatory of Columbia University, 61 Route 9W, Palisades, NY 10964

[2]School of Earth and Environmental Sciences, Queens College and Graduate Center, City University of New York, 65-30 Kissena Blvd., Flushing, NY 11367

[3]U.S. Geological Survey, Maine Water Science Center, 196 Whitten Road, Augusta, ME 04330

[4]U.S. Geological Survey, Branch of Geophysics, 11 Sherman Place, Unit 5015, University of Connecticut, Storrs, CT 06269

[5]Maine Geological Survey, 93 State House Station, Augusta, ME 04333

Abstract

To understand the hydrogeochemical processes regulating well water arsenic (As) evolution in fractured bedrock aquifers, three domestic wells with [As] up to 478 μg/L are investigated in central Maine. Geophysical logging reveals that fractures near the borehole bottom contribute 70–100% of flow. Borehole and fracture water samples from various depths show significant proportions of As (up to 69%) and Fe (93–99%) in particulates (>0.45 μm). These particulates and those settled after a 16-day batch experiment contain 560–13,000 mg/kg of As and 14–35% weight/weight of Fe. As/Fe ratios (2.5–20 mmole/mole) and As partitioning ratios (adsorbed/dissolved [As], 20,000–100,000 L/kg) suggest that As is sorbed onto amorphous hydrous ferric oxides. Newly drilled cores also show enrichment of As (up to 1,300 mg/kg) sorbed onto secondary iron minerals on the fracture surfaces. Pumping at high flow rates induces large decreases in particulate As and Fe, a moderate increase in dissolved [As] and As(III)/As ratio, while little change in major ion chemistry. The δD and $\delta^{18}O$ are similar for the borehole and fracture waters, suggesting a same source of recharge from atmospheric precipitation. Results support a conceptual model invoking flow and sorption controls on groundwater [As] in fractured bedrock aquifers whereby oxygen infiltration promotes oxidation of As-bearing sulfides at shallower depths in the oxic portion of the flow path releasing As and Fe; followed by Fe oxidation to form Fe oxyhydroxide particulates, which are transported in fractures and sorb As along the flow path until intercepted by boreholes. In the anoxic portions of the flow path, reductive dissolution of As-sorbed iron particulates could re-mobilize As. For exposure

© 2014 Elsevier B.V. All rights reserved.

Corresponding author: Yan Zheng, phone 718-997-3329, fax 718-997-3299, yan.zheng@qc.cuny.edu, yzheng@ldeo.columbia.edu.

Publisher's Disclaimer: This is a PDF file of an unedited manuscript that has been accepted for publication. As a service to our customers we are providing this early version of the manuscript. The manuscript will undergo copyediting, typesetting, and review of the resulting proof before it is published in its final citable form. Please note that during the production process errors may be discovered which could affect the content, and all legal disclaimers that apply to the journal pertain.

NIH-PA Author Manuscript
NIH-PA Author Manuscript
NIH-PA Author Manuscript

NIH-PA Author Manuscript

NIH-PA Author Manuscript

NIH-PA Author Manuscript

assessment, we recommend sampling of groundwater without filtration to obtain total As concentration in groundwater.

Keywords

arsenic; domestic well; fractured bedrock aquifer; geophysical logging; pumping test; sorption

1. Introduction

High arsenic (As) concentrations in domestic bedrock wells have emerged as a public health concern in Africa (Kortatsi, 2007; Smedley, 1996; Smedley et al., 2007), Asia (Ahn, 2012; Shukla et al., 2010), Europe (Aloupi et al., 2009; Heinrichs and Udluft, 1999), and Central and North America (Armienta et al., 2001; Ayotte et al., 2003; Boyle et al., 1998; Colman, 2011; Kim et al., 2011; Lipfert et al., 2006; Peters and Blum, 2003; Peters and Burkert, 2008; Pippin et al., 2006; Ryan et al., 2011; Yang et al., 2009), especially in rural areas without public water supply. These bedrock wells typically have low yields and supply small communities or individual households (Drew et al., 2001). Because they are not subject to monitoring or regulatory mandate to meet drinking water quality standards, including that for As, which U.S. Environmental Protection Agency (EPA) has set a Maximum Contaminant Level (MCL) of 10 μg/L, this exposure to As has posed health risks for private well users (Abernathy et al., 1999; Karagas et al., 2002; Rice et al., 2012).

High As occurrence has been reported in the crystalline bedrock aquifers in New England (Ayotte et al., 2003) where 25% population use private wells drilled into fractured bedrocks (Mahler et al., 2005). Previous studies have correlated high As occurrence with bedrock geology at regional (Ayotte et al., 1999; Peters and Burkert, 2008) to local scales (Sidle et al., 2001; Yang et al., 2009), and identified sulfidic minerals, e.g. arsenian pyrite or pyrrhotite, and arsenopyrite, as potential source minerals of As in meta-sedimentary rock formations (Lipfert et al., 2006), with additional plausible sources such as westerveldite (FeAs) and scorodite ($FeAsO_4.2H_2O$) in pegmatite bordering granitic intrusive rocks (Peters and Blum, 2003; Utsunomiya et al., 2003). Geochemical processes, including oxidation of these As minerals, adsorption of As onto oxides/oxyhydroxides or carbonates, and desorption of As into aqueous solution regulated by pH, redox and competitive ions, have been proposed as mechanisms regulating the natural mobilization of groundwater As in fractured bedrock aquifers (Ayotte et al., 2003; Lipfert et al., 2006; Peters, 2008; Yang et al., 2012). Reductive dissolution of As by anthropogenic sources of organic carbon can also enhance the mobility of As in bedrock aquifers (Harte et al., 2012). However, one of the puzzles is that despite the association between bedrock geology and patterns of groundwater As at regional and local scales, As concentrations in bedrock wells could vary greatly from < 1 to 100s of μg/L at the very local scale of < 100 m, i.e. in individual wells. Mixing of high-As reducing/suboxic groundwater and low-As oxic groundwater in fractures and/or in boreholes receiving water from multiple discrete fractures with contrasting groundwater chemistry and redox conditions (Ayotte et al., 2011; Harte et al., 2012) is likely to regulate As concentrations in individual fractured bedrock wells, but these factors have not been explored.

NIH-PA Author Manuscript

NIH-PA Author Manuscript

NIH-PA Author Manuscript

The complexity of flow in inter-connected fractures (Shapiro, 2002) opens the possibility for fluctuation of water chemistry that is difficult to characterize and in turn may cause changes in As concentration in individual wells over time or under different pumping conditions. This conjecture is based on a large body of literature that illuminates the linkage between aquifer transmissivity and chemical transport in the inter-connected fracture network of bedrock aquifers (Johnson et al., 2005; Lane Jr. et al., 2002; Nordstrom et al., 1989; Paillet and Kapucu, 1989). Fractures are heterogeneous in orientation, length, aperture, depth, connectivity, and more importantly, the water producing capacity. The bedrock wells could penetrate fractures with various hydraulic heads, which causes inflows or outflows from different depths in the boreholes. Under varying hydrogeologic conditions, including those induced by pumping, As concentration is hypothesized to respond to changes in flow regime but this has not been evaluated. The changes can be complicated and difficult to predict especially when the rock formations and even various fractures in each well are lithogeochemically heterogeneous, which contribute waters with distinct chemistry such as pH and redox conditions that have been known to influence As mobility. Nevertheless, the large degree of spatial heterogeneity of groundwater As at very local scales may simply reflect connectivity between fractures that yield high As water and those that yield water with little or no As. If this were the case, changes in flow and hence mixing would also result in changes of As levels over time in a given borehole.

To estimate to what extent As concentrations in boreholes reflects a mixture of water derived from various inter-connected fractures, borehole water and fracture water samples (collected using inflatable packers or the dual-pump method that intends to collect samples representative of the fractures) were analyzed for As and other chemical parameters under ambient and pumping conditions in three domestic wells located in the towns of Manchester and Litchfield in central Maine. The wells were chosen to be representative of high As wells in the greater Augusta area where 1,425 wells have been screened for As (Yang et al., 2012; Yang et al., 2009). Geophysical logging was used to characterize fracture zones and to determine flow rates from each zone. Transmissivity of the boreholes and fractures was estimated using pumping tests. Batch experiments using borehole and fracture water samples were conducted to examine effects of reactions occurring in the borehole on dissolved and particulate As and iron (Fe) concentrations over a period of 16 days. Two rock cores were collected in drilled boreholes adjacent to the two aforementioned wells in Manchester and Litchfield and were analyzed for As concentrations in bulk rock and on fracture surfaces. The results shed light on how groundwater flow through the fractures combined with geochemical reactions along these flow paths and in the boreholes affect groundwater As concentrations in boreholes. Such improved understanding will have implications on whether the As concentrations determined from borehole water collected at a random time of a year after limited flushing of the borehole can be used to determine whether or not it is in compliance with the drinking water standard.

NIH-PA Author Manuscript

NIH-PA Author Manuscript

NIH-PA Author Manuscript

2. Material and Methods

2.1 Bedrock wells

Three bedrock wells for domestic use, two from Manchester and one from Litchfield, were selected in the Silurian Waterville Formation (Sw), consisting of interbedded calcareous pelite and sandstone/limestone, that has been shown to display high rates of groundwater As occurrence (Yang et al., 2009). The domestic wells in central Maine are constructed to penetrate glacial overburden into deeper fractured bedrock formations. They are cased from land surface through the overburden such that water is drawn only from fractures in the open boreholes deeper in the bedrock. In central Maine, sand-gravel glacial aquifers with thickness up to 50 meters can be found only in limited geographic areas. These overburden aquifers have relatively high transmissivity with hydraulic conductivity ranging from 10 – 300 meter/day. The bedrock aquifers have lower transmissivity with typical hydraulic conductivity ranging from 8×10^{-5} to 8 meter/day (Harte, 1992; Hsieh et al., 1993; Paillet and Kapucu, 1989). Fractures are widely distributed in the bedrock. The rock formations mostly strike in the NE-SW direction and are nearly vertical, dipping greater than 80 degrees to the northwest or southeast. There are also cross-cutting joints that strike NW-SE and dip steeply based on the field observation of outcrops.

Although both 6-inch diameter bedrock wells in Manchester are located in the Waterville Formation (from the geologic map), they are <0.5 km from the Devonian (D) granitic intrusive rocks (Fig. 1A). Chosen based on a survey of 113 wells in 6 km^2 that found 78% of the wells having > 10 μg/L of As, the total [As] in unfiltered but acidified groundwater from well MA70076 (depth 54.3 m, elevation 88 m) and MA70138 (depth 58.2 m, elevation 85 m) sampled in 2007 were 37.7 μg/L and 73.1 μg/L, respectively. The wells are situated on a slope from the topographic high of the Granite Hill (elevation 149 m), underlain by Devonian granite, to the Lake Cobbosseecontee shore (elevation 52 m) with a regional groundwater flow direction from east to west. The two wells are about 50 meters apart from each other.

A third bedrock well MA70190 (depth 29.6 m, elevation 79 m) from Litchfield (Fig. 1B) was chosen because a survey in 2007 of 49 wells in 5 km^2 detected 57% of the wells had > 10 μg/L of As and the highest total [As] of 478 μg/L was in this well water. It is also located in the Waterville Formation.

All the three wells were used regularly for domestic supply by the homeowners, and were only discontinued during the field work of this research.

2.2 Geophysical logging

Caliper and fluid conductivity loggings (Mount Sopris Instruments, 2PCA-1000F) were conducted to determine the well depth and the length of well casing, as well as the depths of fractures, which can be determined from changes in well diameter, water temperature, and/or specific conductance. Acoustic televiewer logging (Advance Logic Technology, ABI40) was used for vertically profiling the borehole, providing information regarding the depth and orientation of fractures. Optical televiewer logging (Advance Logic Technology, OBI40) was carried out in well MA70190 to obtain images to better identify formations and

NIH-PA Author Manuscript

NIH-PA Author Manuscript

NIH-PA Author Manuscript

fractures. Heat-pulse flow meter logging (Mount Sopris Instruments, HPFM-2293) was performed to measure flow rates under ambient and pumping conditions and to determine the proportion of water contribution from or to the fractures at various depths.

2.3 Pumping test and water sampling

Pumping tests were carried out to estimate borehole transmissivity following the Cooper-Jacob straight line method (Cooper and Jacob, 1946). Water table drawdown and recovery were recorded manually by a water-level meter and continuously by a pressure transducer (Solinst Levelogger model 3001). Borehole water samples were also collected over the course of pumping tests under stressed conditions.

Pilot pumping tests were conducted in 2008 in the two Manchester wells under high and varying flow rate conditions (15.9 L/min for 2 hours, or 2.1 borehole volume in well MA70076, 7.9 – 31 L/min for 7 hours, or 5.7 borehole volume in well MA70138, Tables 1–2). Borehole water samples (named with an initial “P”) were collected using the extraction pump from shallow depths right below the water table in the wells (P70076.0 from 30.5 m in well MA70076, P70138.0 at the land surface in artesian well MA70138) in the beginning of the pumping tests, and were from the bottom of wells (P70076.1 from 52 m in well MA70076, P70138.1 and P70138.2 from 57 and 52 m, respectively, in well MA70138) towards the end of the pumping tests.

Pumping tests with constant flow rates were conducted in all three wells in 2009 and 2010 (Tables 1–3). Pumping at 3.7 L/min for 3.5 hours at 30 m depth in well MA70076, 9.1 L/min for 2 hours at 35 m depth in well MA70138, and 5.3 L/min for 3.5 hours at 29 m depth in well MA70190, was carried out to pump water of ~ 1 borehole volume. Borehole water samples (named with an initial “B”) were collected every 1 – 1.5 hours during the pumping tests.

After the pumping tests, fracture water samples (named with an initial “F”) were collected from selected depths where fractures were identified by geophysical logs in each well, from greater to shallower depths (Tables 1–3). A dual-pump technique, with one pump placed below the well casing and pumped at higher rates to keep the borehole flushed and a second pump placed at the desired sampling depth to draw water at lower rates, was applied for wells MA70076 and MA70138. In well MA70190, two inflatable packers (Roctest, model YEP) were positioned and inflated to collect water samples from specific 1.5-m fracture intervals (packed volume 27 L) after 1.4 – 6.9 times of packed volume were extracted (Table 3). Fracture water samples were collected after the pH, dissolved oxygen and specific conductance (simultaneously monitored using a YSI 600QS multiprobe in a flow cell) had stabilized.

For all the above water sampling events, four aliquots of samples were collected. The 1st aliquot was filtered through a 0.45-μm membrane filter into a HDPE vial and then acidified to 1% nitric acid (HNO_3, Optima grade) for cation analysis. The 2nd aliquot was also filtered but not acidified for anion analysis. An arsenic speciation cartridge (retains negatively charged As(V) but allows neutral As(III) to pass through, from Metalsoft Center, NJ) was attached after the filter to collect the 3rd aliquot for dissolved arsenic (III) analysis (acidified

NIH-PA Author Manuscript

NIH-PA Author Manuscript

NIH-PA Author Manuscript

after collection). The 4th aliquot was the unfiltered water sample, sometimes with visible iron-rich particles, that was later digested with HNO_3 (Optima grade) for total As analysis. An additional filtered aliquot of each water sample was collected for H and O isotope analysis from well MA70190. Groundwater pH, dissolved oxygen and specific conductance were monitored during sampling.

Twenty-five private bedrock wells in central Maine were sampled in 2013 to estimate the difference between unfiltered and filtered well water [As] and [Fe] (Flanagan et al., In press). All samples were collected when the temperature, pH, dissolved oxygen and specific conductance were stable, typically after running the well pump for 15–30 minutes. Filtered samples were collected through a 0.45-μm membrane filter into HDPE vials and then acidified to 1% nitric acid (HNO_3, Optima grade) for As and Fe analysis.

2.4 Batch experiments

Batch experiments were conducted to evaluate reactions that can modify total and dissolved [As] of groundwater in the boreholes. Unfiltered borehole water (from shallow depths) and fracture water samples (from depths near the bottom) from Manchester wells MA70076 and MA70138 were collected into cubitainers (Hedwin, LDPE, 4 L) at the end of pumping tests. For each sample, two cubitainers were filled, placed in thick-walled black plastic bag immediately, and kept in dark for the duration of the experiments. One cubitainer was kept sealed while another was continuously purged with air intended to promote oxidization. The same suite of 4 aliquots were collected at each of the 7 time points, i.e. in 8 and 16 hours, 1, 2, 4, 8 and 16 days. Again, pH, specific conductance and dissolved oxygen in cubitainers were recorded during sampling.

At the end of the experiments, the entire volume of water and particles in the cubitainers were filtered through 0.7 μm glass fiber filters (Whatman GF/F). The particles together with filters were dried and weighed, then digested by concentrated HNO_3 (Optima grade) on a hot plate. The digests were diluted and analyzed for As, Fe, P, S and Mn.

2.5 Analytical methods

Major anions, including Cl^- and SO_4^{2-}, in water samples were analyzed using Ion Chromatography (Dionex DX500) following the EPA method 300 at Queens College. Alkalinity was measured using the Gran titration method. Major cations and trace elements, including As, were analyzed using the High Resolution Inductively Coupled Plasma Mass Spectrometry (VG Elemental, Axiom) (Cheng et al., 2004) at Lamont-Doherty Earth Observatory. H and O isotopes were analyzed by a gas-source isotope ratio mass spectrometer (Finnigan Delta S) using VSMOW for standardization in the Environmental Isotope Laboratory at the University of Arizona.

2.6 Rock cores

Two continuous sets of bedrock cores were collected from newly drilled boreholes (3-inch diameter) adjacent to the Manchester well MA70076 (N44.30498, E-69.87825, 27.7–47.6 m below ground) and Litchfield well MA70190 (N44.18458, E-69.93929, 15.4–46.3 m below ground). As and Fe concentrations in bulk rock sections and fracture surfaces of core

NIH-PA Author Manuscript

NIH-PA Author Manuscript

NIH-PA Author Manuscript

samples were analyzed using Innov X handheld XRF that has a detection limit of ~ 12 mg/kg for As.

3. Results

3.1 Lithology and fractures of boreholes

The Manchester core, collected in the vicinity of well MA70076, indicates that the fractured bedrock aquifer is beneath 27.7 m of till, which is cased off in the well (Fig. 2). The underlying 27.7–47.6 m is composed mainly of coarse grained granite. Pegmatite with feldspar and rusty weathered pyrite and/or iron oxide on the fracture surfaces are observed at various depths. The weathered fracture surfaces within core sections at depths of 27.7–29 m, 31–33 m, and 40–44 m show >100 mg/kg of As (up to 700 mg/kg) and up to 16% weight/weight of Fe. In contrast, freshly cut bulk rock surfaces (n=23) show As concentrations below the detection limit of ~12 mg/kg. A felsic vein at ~40 m depth in the pegmatite section shows 19 mg/kg of As. Geophysical logs suggest three fracture zones in well MA70076. The first is a group of high angle fractures just below the casing from 28.3 to 34 m depth, indicated by large variations in well diameter from the caliper log, fluid resistivity (not shown) and specific conductance. The second fracture zone is a bundle of horizontal fractures between 36 and 41 m depth. The third zone includes the deep fractures from 47 m depth to the bottom of the borehole where water temperature and fluid conductivity reach maximum values.

Well MA70138 located in Manchester also shows three major fracture zones (Fig. 3). The shallow fracture zone is from 32.1 m (the bottom of the casing) to 36 m depth characterized by many open fractures as indicated by abruptly enlarged well diameters. The second fracture zone is between 37 and 52 m depth with many fractures, the orientations of which vary and do not appear to have a consistent pattern. The deep fracture zone is from 53 m to 58.2 m (the well bottom) with large fractures corresponding to sudden increases of fluid conductivity.

Drilling for the Litchfield core, in the vicinity of well MA70190, penetrated 15 m-thick upper layer of till, a rusty weathered granite unit between 15 and 24 m, and interbedded calcareous pelite and sandstone/limestone of the Waterville Formation from 24 to 46 m (Fig. 4). The core sections of 18–19 m, 22–24 m, 27–33 m, and 41–45 m show >100 mg/kg of As (up to 1,300 mg/kg) and up to 50% w/w of Fe on rusty weathered pyrites and/or iron oxides on the fracture surfaces. In comparison, freshly cut bulk rock surfaces (n=25) show As concentrations below the detection limit of ~12 mg/kg except one reading of 44 mg/kg at 45.17 m. The geophysical logs in well MA70190 (29.6 m deep) show high angle fractures from 19.2 m (bottom of the casing) to 22 m in rusty weathered granites and at the contact between the Devonian granite and the underlying Waterville Formation at 24.4 m. There are vertical fractures between 25.1 and 26.7 m and a deep zone of three horizontal fractures at 26.8 – 27.4 m.

NIH-PA Author Manuscript

NIH-PA Author Manuscript

NIH-PA Author Manuscript

3.2 Borehole transmissivity and water producing fractures

The borehole transmissivity estimated from the water level recovery data during the pumping tests is 0.31 square meter per day (m^2/d) for well MA70076, 0.40 m^2/d for well MA70190, with well MA70138 showing a very high value of 10.6 m^2/d (Fig. 5). These estimated borehole transmissivity values are comparable to those determined in similar bedrock units in New England, e.g. 0.46–2.8 m^2/d in Bigelow Brook Formation of meta-sedimentary sillimanite gneiss in Storrs, CT (Johnson et al., 2005); 0.19–8.0 m^2/d in a fractured granitic gneiss and micaceous schist formation of Cambrian-Ordovician age in Norwalk, CT (Lane Jr. et al., 2002); and 0.01–10 m^2 /d in Mirror Lake, NH, where the bedrock is pelitic schist intruded by granite and overlain by glacial drift and where most boreholes have at most 2 or 3 highly transmissive fractures (transmissivity > 0.1 m^2/d) (Paillet, 1998; Shapiro, 2001).

In all three wells, the fractures supplying most of the water to the boreholes are at depths near the borehole bottom, as indicated by the most significant increase of inflow rates under ambient (well MA70138, Fig. 3) or pumping conditions (wells MA70076 and MA70190, Fig. 2&4). This is consistent with the practice that drillers usually stop drilling and complete well installation at depths where productive fractures with sufficient yields are encountered. In well MA70076, almost all of inflow into the borehole comes from the deepest fracture zone below 47 m, with fractures at the very bottom contributing 70% of inflow. In the artesian well MA70138 with an ambient flow rate of approximately 7.6 L/min, the deep fractures below 53 m are estimated to contribute more than 70% of water inflow to the borehole. In well MA70190, 26% of inflow is estimated to come from the bottom fractures, and 66% from the deeper horizontal fractures below 26.8 m, while the shallow high-angle fractures (19–22 m) only contribute 8% of flow into the borehole.

3.3 Dissolved and particulate As in borehole and fracture water

In all three boreholes, dissolved As concentrations in fracture water are > 10 μg/L (Figs 2–4) but can be significantly less than the total As concentrations (Tables 1–3), suggesting that groundwater As consists of both dissolved and particulate (> 0.45 μm) forms in the fractures before entering the borehole. When total As concentration is > 1,000 μg/L with simultaneously high total Fe concentration of > 10 mg/L, this release of Fe-particles from the open borehole is most likely attributed to disturbance by the deployment of sampling equipment and thus not considered in this description of results (see also section 3.4 below). These aggregated particles tend to be large and visible. In comparison, most samples were collected when the water was visibly clear without apparent aggregates.

Because the dual-pump technique was used to sample fracture water in MA70076 and MA70138, there is a possibility that some borehole water was entrained and mixed into the fracture water samples, more so for the high transmissivity well. Indeed, MA70138 with high transmissivity has a nearly uniform dissolved As concentration (50.7 – 54.4 μg/L) regardless of fracture depth sampled (Fig. 3). Intra-borehole flows that result in mixing of borehole water into fracture water under ambient conditions (Mack et al., 2011) could contribute to entrainment for MA70138 because the purging period is not long enough due to high transmissivity. In MA70076, dissolved As concentrations vary from 24.7 μg/L at 30

NIH-PA Author Manuscript

NIH-PA Author Manuscript

NIH-PA Author Manuscript

m to 36.7 μg/L at 54 m depth (Fig. 2). This slight variation with depth is consistent with a well of low transmissivity and likely low intra-borehole flow, with the high dissolved As water from bottom fractures being diluted to a larger extent towards the shallower depths by borehole water or other inflow water with lower dissolved As. In both Manchester wells, the water producing fractures at the greatest depths yield water with dissolved As concentrations that are similar to those of the borehole water at the end of each pumping test (Tables 1–2). More remarkably, however, these fractures also yield water with variable and often higher total As concentrations than those of the borehole water at the end of the pumping (Tables 1–2). This might suggest that pumping has induced the transport of water with fairly constant dissolved As concentrations but with more variable total As concentrations from the fractures, although we cannot rule out the disturbance by sampling equipment.

The likelihood of borehole water entrainment to fracture water in MA70190 is much less due to the employment of packers for sampling. There is also little ambient flow (Fig. 4), suggesting low intra-borehole flow. Interestingly, the water producing fractures at the greatest depths yield water with total and dissolved As concentrations lower than those of the borehole water at the end of the pumping test (Table 3). This suggests that other low water producing fractures with higher As concentrations might exist but were not captured during our sampling.

Despite the differences among the three wells, the results show that water producing fractures at the bottom of each borehole can be dominant sources of both dissolved and particulate As to the well water, consistent with previous findings (Ayotte et al., 2011).

Rock core As depth profiles also are consistent with a source of As at the bottom of the boreholes. For the rock core collected in the vicinity of well MA70190, the 29–33 m zone shows pronounced As enrichment on fracture surfaces and is corresponded to the high dissolved and total As concentrations observed in the fracture water samples collected using inflatable packers (Fig. 4). There is also rock As enrichment on fracture surfaces between 27–28 m. These two depths also dominate the water inflow to the borehole. Thus, for MA70190 with the highest groundwater As concentration in our survey of 1,425 wells in central Maine, it appears that fractures with high flow rates coincide with very high levels of As in fracture surfaces, and may have been mobilized through reductive dissolution (Gotkowitz et al., 2004; Kim et al., 2003). Unfortunately, the core collected at MA70076 in Manchester did not penetrate to the depth of the borehole bottom with water producing fractures (Fig. 2). Nevertheless, high As on fracture surfaces at 27.5–33 m and 40–44 m depth intervals are observed, although these fractures most likely do not currently contribute As to well water due to very limited flow from these intervals (Fig. 2).

Despite the difference of dissolved and total As concentrations in fracture and borehole waters, the major cation and anion compositions are mostly similar in each well sampled in different years and from various pumping depths (Tables 1–3). Additionally, very narrow ranges of δD (−64.5 to −62.4‰) and $\delta^{18}O$ (−9.82 to −9.64‰) are found in fracture and borehole water samples of well MA70190 (Table 3). The D/O isotopic data of MA70190 fall onto the local meteoric water line (LMWL) of $\delta D=7.35\delta^{18}O+6.8$ based on rain and snow data (Sidle, 2003). This suggests recharge by atmospheric precipitation. The $\delta^{18}O$ values are

NIH-PA Author Manuscript

NIH-PA Author Manuscript

NIH-PA Author Manuscript

similar to those in fractured bedrock groundwater from Northport, Maine (−9.5 to −8.3‰) (Lipfert et al., 2007) and the Goose River basin (−12.1 to −8.8‰) of mid-coastal Maine (Sidle, 2002) where young groundwater with ages less than 50 years was found in about 31–37% of sampled wells based on ^{3}H and ^{85}Kr analyses (Sidle and Fischer, 2003).

The results suggest that borehole and fracture waters are derived from the same source sharing flow paths through rocks that are highly variable in As composition.

3.4 Pumping induced particulate and dissolved Fe, As and As(III) change

Particulate As and Fe concentrations can be calculated by taking the difference between the total and dissolved concentrations. Despite high particulate Fe concentrations of mg/L levels in borehole and fracture waters, the dissolved Fe concentrations are usually very low (<0.1 mg/L), especially when only considering samples with < 10 mg/L particulate Fe (Tables 1–3) that are not disturbed by sampling equipment. Particulate Fe concentrations declined from > 10 mg/L in the first samples obtained during the pumping tests hence subjected to the most disturbance, to 1–2 mg/L towards the end of the pumping tests after ~1 borehole volume was replaced (Fig. 6). The dissolved Fe concentrations in the two Manchester wells even decreased to < 0.01 mg/L towards the end of pumping (Fig. 6). The dissolved Fe in the Litchfield well experienced fluctuation but eventually declined to 0.09 mg/L (Table 3). Fracture waters also contain much lower amounts of dissolved Fe compared to particulate Fe (Tables 1–3). It is noteworthy that the water-producing, As-bearing fractures at the bottom of three boreholes all yielded water that contained not only higher dissolved Fe but also higher particulate Fe than those collected at the end of pumping tests in the boreholes. Furthermore, the sum of major ions and specific conductance were near constant during pumping tests in each well (Tables 1–3) despite large changes in particulate Fe, which in part is attributed to cleaning out of disturbed Fe particles from the borehole as pumping progressed.

Particulate As concentrations also decreased with the pumping time, similar to the trend for particulate Fe concentrations in each well (Fig. 6). On the other hand, dissolved As concentrations increased with pumping, suggesting that the fracture waters with higher dissolved As concentrations than borehole water are entering the borehole. Consistent with this, the dissolved As(III)/As ratios also increased during pumping. This is especially evident for well MA70190 that the dissolved As(III)/As ratios increased from 55% to ~100% over 210 mins of pumping at 5.3 L/min (Fig. 6 and Table 3). At the low pumping rates used in 2009 pumping tests, dissolved As(III)/As ratios did not change for the two Manchester wells (Fig. 6). However, pumping at 15.9 L/min in 2008 for 113 minutes resulted in a dissolved As(III)/As ratio of 10% for MA70076 at the end of pumping (Table 1). Pumping at 7.9 and then 31 L/min for 550 mins in 2008 resulted in a dissolved As(III)/As ratio of 11–20% for MA70138 at the end of pumping (Table 2). These higher pumping rates used in 2008 yielded waters with similar chemistry, total and dissolved As concentrations as those samples collected in 2009 using lower pumping rates (Tables 1 and 2). It is worth noting that after the longest pumping time of 550 min at the highest rate of 31 L/min, dissolved and total As concentrations are comparable for MA70138 (sample P70138.2, Table 2), although Fe is still dominated by particulate Fe. Thus, it is likely that As

NIH-PA Author Manuscript

NIH-PA Author Manuscript

NIH-PA Author Manuscript

in fracture water at the very beginning of the flow path may be more dominated by As(III) and is in dissolved form, although this is difficult to ascertain because the low transmissivity of the fractures prevents prolonged pumping at high rates.

3.5 Association between particulate As and Fe

At the end of the pumping tests, the As/Fe ratios of borehole water particulates become comparable with those of the fracture water particulates (Tables 1–3). The As/Fe ratios of particulates in the last borehole water samples were 2, 5 and 28 mmole/mole for MA70076, MA70138 and MA70190, respectively. The results also suggest that although fracture water inflow is endowed with As-rich Fe particles, there is further As sorption to these Fe particles after the water enters the borehole because the average As/Fe ratios of particulates in the borehole water with minimal pumping were higher than those in the fracture waters in all three wells.

Without further investigation of Fe mineralogy of the particulate matter in the borehole and fracture waters, the reasons for the very different As/Fe ratios in these particles cannot be determined. This difference is again evident in particles sampled over time in batch experiments (Table 4) and in the settled particles collected at the end of the batch experiments (Table 5). All three well waters were slightly alkaline with pH between 7 and 8, and are of Ca^{2+}-HCO_3^- type. Borehole waters tend to be oxygenated. However, pumping indeed lowered the dissolved oxygen level in MA70190 to 0.7 mg/L and all dissolved As was then dominated by As(III). The other two boreholes remained oxygenated, but MA70138 showed a decline in dissolved oxygen to 0.7 mg/L with 20% dissolved As as As(III) at the end of the pumping test in 2008 using high pumping rates. Thus, it appears that sorption of dissolved As to Fe-particles has occurred along the flow path in the fractures.

Because the dissolved Fe concentrations in all types of water were low, the batch experiments are not a good model system to observe Fe oxidation and formation of Fe-particles. It is also not a good model system to observe As oxidation because experiments were conducted only in two Manchester wells using water that was dominated by As(V) (Table 4). Nevertheless, the tiny amount of dissolved Fe in the waters did all become Fe-particles because concentrations of dissolved Fe decreased to ~ 0.001 mg/L in 8 experiments (Fig. 7). Particulate Fe was present in the water samples at high concentrations at the beginning of the experiments. Both particulate As and Fe followed the logarithmic decrease trend over 16 days. These suspended As-loaded Fe particles tended to settle down slower in experiments with air purging (estimated settling half time of 0.5–0.8 days) than in those without (estimated settling half time of 0.15–0.35 days). This is because the continuous disturbance from air purging kept the particles suspended in solution. Dissolved As showed very little change over 16 days. The final dissolved As concentrations towards the end of experiments were slightly higher in air-purged settings than those without in the 4-pairs of experiments, which is probably due to the higher pH in the air-purged samples at the end of experiments that favored less sorption of As. This slightly higher pH in air-purged experiments might be caused by the purging of dissolved CO_2.

NIH-PA Author Manuscript

NIH-PA Author Manuscript

NIH-PA Author Manuscript

4. Discussion

4.1 Arsenic sorption to hydrous ferric oxides particles

Previous studies of fractured bedrock aquifers in the region have highlighted the importance of As-rich primary minerals in rock formations as a source of As to groundwater and suggested the association between arsenic and iron oxyhydroxides in these aquifers during mobilization (Ayotte et al., 2003; Lipfert et al., 2006; Peters and Blum, 2003; Sidle et al., 2001; Utsunomiya et al., 2003). Here, multiple lines of evidence point to a large reservoir of As sorbed onto presumably secondary Fe minerals that not only has coated the fracture surfaces but also has been transported along the fractures to enter the boreholes.

The precipitated particles at the end of batch experiments were highly enriched in Fe averaging 23% in weight (range: 14%–35%), which is significantly lower than 63% in goethite (α-FeO(OH)) or 58% in six-line ferrihydrite ($5Fe_2O_3 \cdot 9H_2O$), but comparable to 6–26% in the iron-rich incrustations (mostly amorphous ferrihydrite) observed in 26 bedrock wells in the Schwabach field near Nuremberg, Germany (Houben, 2003) and 25% for bulk particles (up to 37±3% in the surface 1 μm depth) in amorphous HFO synthesized in laboratory (Jang et al., 2006).

In Manchester well MA70076, As concentrations in particles range from 780 to 1,180 mg/kg in batch experiments (Table 4), and are from 560 to 1,480 mg/kg during pumping tests and fracture sampling (Table 1). In Manchester well MA70138, they are from 1,570 to 3,020 mg/kg in batch experiments (Table 4) and from 1,580 to 2,380 mg/kg during pumping tests and fracture sampling (Table 2). In Litchfield well MA70190, they are from 3,620 to 12,600 mg/kg during pumping tests and fracture sampling (Table 3). Particle As concentrations during pumping tests and fracture sampling were estimated by applying an average Fe weight ratio of 23% in particles. These As concentrations are comparable to those (~1,000 mg/kg at equilibrium with ~40 μg/L dissolved As(V) at pH 7–8, ~6,000 mg/kg at equilibrium with ~300 μg/L dissolved As(III) at pH 8) in laboratory experiments of As adsorption on amorphous HFO. But they are much higher than those (~70 mg/kg at equilibrium with ~40 μg/L dissolved As(V) at pH 7–8, ~600 mg/kg at equilibrium with ~300 μg/L dissolved As(III) at pH 8) of As sorbed onto goethite (Dixit and Hering, 2003).

The average As/Fe ratios of particulates in the fracture water samples were 2.5±0.4 (pH 7.1–7.2), 6.0±1.0 (pH 7.4–7.8), and 20±5 (pH 7.6–8.0) mmole/mole for MA70076, MA70138 and MA70190, respectively. These ratios are comparable to those reported As/Fe ratios in freshly precipitated ferric hydroxides (11 mmole/mole) (Kim and Nriagu, 2000) and under equilibrium of adsorption on ferric hydroxides (~40 mmole/mole As(V) at 50 μg/L [As(V)] and pH 6.8, ~11–75 mmole/mole As(III) at 100–300 μg/L [As(III)] and pH 6.8–9) (Meng et al., 2000).

Another line of evidence supporting the sorption of As onto Fe-rich particulates is the apparent partitioning ratio (Xd, Tables 1–3) for As, defined as adsorbed As concentration on $FeO(OH) \cdot nH_2O$ divided by dissolved As concentration in water. The Xd values in the three wells were 20,000 to 100,000 L/kg, much higher than the typical As adsorption coefficients (Kd) on natural sediments based on batch experiments, which are only a few to at most 10s

NIH-PA Author Manuscript

NIH-PA Author Manuscript

NIH-PA Author Manuscript

L/kg under equilibrium (Jung et al., 2012; Radloff et al., 2011). However, they are more comparable to those (1,000,000–3,000,000 L/kg for As(V) and 100,000–500,000 L/kg for As(III)) of synthetic ferric hydroxides of laboratory experiments at pH 6.8 (Meng et al., 2000). These high Xd values indicate the iron particulates in Maine groundwater are probably thermodynamically unstable amorphous ferrihydrite. If so, they will have very large surface areas (150–400 m^2/g) (Houben, 2003) and possibly in nanometer-sized ferrihydrite crystallite forms (Jessen et al., 2005) as found in the early stage of precipitation where groundwater containing ferrous iron is aerated (Jambor and Dutrizac, 1998), even without visible particles in the water. The decrease of the Xd values during pumping tests in wells MA70076 and MA70138 is probably because the freshly supplied fracture water did not reach adsorption equilibrium. The lower partitioning ratios in borehole water of well MA70190 during the pumping test are probably due to the slower adsorption of As(III) compared to AS(V) (Raven et al., 1998) in this well (dissolved As(III)/As 55–100%, compared to 0–11% in two other wells). Additionally, the desorption of As is favored by higher pH as well (Ghosh and Yuan, 1987; Pierce and Moore, 1982).

Thus, As and Fe concentration ranges, As/Fe ratios in the particles of borehole and fracture water, as well as the partitioning ratios of As between the particles and water, suggest that the Fe-particles are most likely in the mineral form of amorphous HFO and that the As is sorbed onto HFO.

4.2 Flow and sorption regulate groundwater As

We propose here a conceptual model (Fig. 8) to illustrate how As is mobilized from the dispersed primary mineral source in meta-sedimentary rocks to its occurrence as dissolved and particulate As in borehole water fed by water-producing fractures, taking into account the new finding here that As and Fe exist as particulates in fractures, and may also transport along the fractures. In this model, infiltration of oxygen into the shallower depths of the aquifer promotes oxidation of As-bearing sulfides in the oxic zone, releasing As(III) as $As(OH)_3$ and Fe(II) as Fe^{2+}8. The oxidation of Fe(II) by oxygen to form amorphous HFO is usually very fast with a half time of <0.5 to 2.5 hrs under even neutral pH conditions (Davison and Seed, 1983; James and Ferris, 2004; Kim and Nriagu, 2000). The newly formed particulate Fe is likely to be of colloidal form or nanoparticles (Bauer and Blodau, 2009; Gunnars et al., 2002; Guo et al., 2011; Liu et al., 2011; Pedrot et al., 2011; Pullin and Cabaniss, 2003; Stolpe et al., 2013; Thompson et al., 2006; Wolthoorn et al., 2004), and will take time to aggregate to form particles large enough to settle. These smaller, suspended particulate Fe can be transported along the fracture flow path. Because not all pyrites are enriched in As but all have Fe as a major component, there will be Fe particles that are low in As content depending on each particle's source. The freshly formed Fe particles can also sorb more As along the flow path if more As was liberated from additional sources, such as oxidation of pyrites and desorption from less amorphous Fe oxyhydroxides on fracture surfaces. It is conceivable that sorption of both As(III) and As(V) onto Fe particles occurs along the flow path until it is intercepted by a borehole, and may continue in the borehole. This is because the oxidation of As(III) to As(V) as $H_2AsO_4^-$ by oxygen under circum-neutral pH conditions is slower (half time of a few hours to several days) (Amirbahman et al., 2006; Hug et al., 2001; Hug and Leupin, 2003; Kim and Nriagu, 2000) than that of Fe(II)

NIH-PA Author Manuscript

NIH-PA Author Manuscript

NIH-PA Author Manuscript

and may accelerate under microbial influence (Katsoyiannis and Zouboulis, 2004; Wilkie and Hering, 1998). Sorption of As(III) has a half time of 1–5 hours (Giménez et al., 2007; Katsoyiannis et al., 2008; Lenoble et al., 2002) or longer (>1 day) with the existence of competitive negatively charged function groups such as SO_4^{2-}, HPO_4^{2-}, and humic acid (Ko et al., 2004). It is worth noting that the sorption capacity is lower for As(III) than that for As(V) (Dixit and Hering, 2003; Goldberg, 2002; Lin and Puls, 2000).

As the water flows farther down the flow path and away from the oxic zone, the oxidation of As-bearing sulfides is expected to continue in the suboxic zone until the oxygen is depleted, although the reaction rates may differ. At present, we do not know whether there are anoxic zones or pockets in the aquifer. It is conceivable that small fractures poorly connected to the large fractures contain reducing groundwater because pumping at high rates have drawn out water with lower oxygen and more As(III). However, this possibility is very difficult to ascertain because pumping is presumably drawing more water from the preferential flow paths in the aquifer system, i.e. large fractures that are better connected than from the poorly connected small fractures. Thus remobilization of As from reductive dissolution of these Fe particles is a possibility that cannot be ascertained yet. What is evident is that the borehole itself represents a significantly more oxygenated environment than groundwater flowing along the deeper fractures in the suboxic zone (Fig. 8).

Considering this oxic-suboxic(-anoxic)-suboxic-oxic gradient along the groundwater flow path and into the borehole (Fig. 8), this conceptual model would predict, a) boreholes that intercept fractures having the longest flow path and hence a higher likelihood of interacting with As-rich primary minerals in the earlier part of the flow path that is oxygenated, are likely to be enriched in As in both dissolved and particulate forms; b) this process of secondary As enrichment on fracture surfaces does not need to be contemporary and could reflect historical change in groundwater flow and hydraulic regime that may have impacted how deep oxygen penetrated into the subsurface in the geologic past.

Is there a possibility that the differences in particulate As/Fe ratios observed in the three boreholes reflect how long the Fe particles have been traveling along the flow path, allowing time to load As? This may be the case for MA70076 and MA70138 that are within 50-m of each other hence share similar lithology, with one down gradient from the other. However, it cannot be excluded that the much higher particulate As/Fe ratios at MA70190 in Litchfield reflect higher concentrations of As in the primary mineral sources in the bedrock. Future studies are needed to explore whether more As is sorbed onto Fe particles down the flow path and whether the truly dissolved (solute) As concentrations in groundwater are controlled by sorption equilibrium with As-sorbed Fe particles that are ubiquitous in the aquifer.

The fracture water from various depths showed different As partitioning ratios, particularly in well MA70190 (Table 3) where fracture water samples were collected from packer-sealed intervals and thus are better representative of fracture environments, barring the limitation of an inherent sampling bias to better connected fractures under pumping. The dissolved As concentration in fractures is considered to be further regulated by the specific conditions, such as pH, redox, and iron chemistry in individual fractures. An interesting observation is

NIH-PA Author Manuscript

NIH-PA Author Manuscript

NIH-PA Author Manuscript

that dissolved As concentrations from the fracture waters were less than the dissolved As concentrations in borehole waters towards the end of the pumping tests. This is probably due to the quick As oxidation and adsorption (Raven et al., 1998) in the pumping pipe and the sampling flow cell, which could be reflected by the high DO concentrations recorded by the YSI connected with the flow cell during fracture specific water sampling. The low flow rates from specific fractures that caused longer sampling time might also contribute to the oxidation and adsorption of As and thus lower dissolved [As].

4.3 Implications for groundwater sampling and household water use

That a very large proportion of Fe and to a lesser extent As is associated with HFO particulates in groundwater from the three wells tested in this study implies that groundwater Fe and As concentrations reported in our previous studies (Yang et al., 2012; Yang et al., 2009) may reflect both particulate and dissolved components because unfiltered well water samples were collected for the evaluation of groundwater As occurrence in central Maine. The concentrations of As in unfiltered samples are systematically higher by 11% than those of filtered (0.45 μm) samples when 43 water samples in bedrock wells in New England were analyzed (Ayotte et al., 2003). In another study of crystalline bedrock wells in mid-coast Maine, 20% of the water samples (n=30) showed As concentrations that were at least 10% higher in the unfiltered samples than those in the filtered ones, and 57% of the same water samples had total Fe concentrations more than 10% higher than dissolved Fe concentrations (Lipfert et al., 2006). A sampling of 25 household well water in central Maine revealed that As concentrations in unfiltered water are on average 5% higher than those filtered, while Fe concentrations in unfiltered water are on average 70% higher than dissolved Fe concentrations, with 50% of the well water samples show at least 100% higher in unfiltered water (Fig. 9). The typical household well water sampling for exposure assessment usually collect water samples at low flow rates, and thus only collect a small fraction of the borehole water (10s of L out of 500–1500 L) that sat for a relatively long time with most As-rich iron particles settled down to the borehole bottom. It is also known that colloidal Fe can result in an overestimation of dissolved Fe since 0.45 μm filter used to separate the dissolved form from the particulate form does not, by definition, remove particles in colloidal forms Bauer and Blodau, 2009). If colloidal Fe is present in large quantity, then using a 0.45 μm filter to assess dissolved As concentration also likely leads to an overestimation of dissolved As levels because of As-Fe colloids association has been demonstrated in As-rich groundwater from the Hetao Plain of Inner Mongolia, China (Guo et al., 2011). In addition, disturbance of Fe particles in the borehole by sampling equipment can also introduce As-rich Fe particles into groundwater samples, making interpretation difficult because there are considerable variations in As/Fe ratios in these particles. The association between Fe and As in groundwater, particularly those groundwater samples with extremely high Fe but low As could be affected by the presence of particulate or colloidal Fe.

To filter or not to filter is a question worthy of discussion when it comes to exposure assessment of groundwater As. Because the particulate As in groundwater from such aquifers is likely to be affiliated with amorphous HFO, and that the stomach acids are expected to dissolve such particulate As (Hamel et al., 1998), this As is largely bioavailable. Filtering well water through a 0.45 μm filter while collecting water samples for exposure

NIH-PA Author Manuscript

NIH-PA Author Manuscript

NIH-PA Author Manuscript

assessment could contribute to some false negatives, e.g., more samples will be found to meet Maximum Contaminant Level of As (10 μg/L) because only the "dissolved" As is being measured. We suggest that until the health effects of such potentially bioavailable particulate As in groundwater are investigated and found to be different from the dissolved As, it is prudent to determine total As concentrations of well water samples by acidifying the samples to 1% HNO_3 and allow for approximately 1 week of reaction time to ensure all particulate As has been dissolved before measurement.

In our study area consisting of 17 towns in central Maine, the yields of private bedrock wells ranged from 1 to 1000 L/min based on well owners' reports (n=376), with an average yield of 53 L/min and a median value of 23 L/min. Given the average per capita use for self-supplied domestic water is 223 L/day in Maine (Kenny et al., 2009), and the average household size of 2.34 (Census, 2010), the daily water demand from each household, similar to daily water extraction from each well, is 520 L. This is equivalent to 10–25 min of pumping. This period of pumping extracts mostly borehole water, which could contain substantial amounts of particulate Fe and As (mainly As(V) if the well water is more oxic), or As(III) if the well water is more reducing/suboxic. A household treatment system with oxidation and adsorption capacity is thus more likely to effectively remove As.

About 40% of 307 private well owners in our study area have installed sediment filters, although many of them report that the filters have not been changed or maintained since the initial installation. How effectively a sediment filter can remove the particulate Fe and the associated As requires further assessment. When homeowners submitted their drinking water for water quality tests to the state laboratory for As analysis, 48% provided no information on whether they used water treatment or not, about one quarter reported that they used some forms of water treatment, and about another quarter reported that they did not (Nielsen et al., 2010).

5. Conclusions

Geophysical logging and pumping tests in three domestic wells drilled into fractured bedrock aquifers in central Maine reveal that groundwater containing As typically comes from the high yielding fractures near the bottom of boreholes. In both borehole and fracture waters from the 3 wells tested, the majority of Fe is in the form of particulate matter that also is found to have sorbed a considerable amount of As. Pumping tests and batch experiments that evaluated the As and Fe contents of the particulates, As partitioning and dissolved As speciation support that flow and sorption control groundwater As in fractured bedrock aquifers with meta-sedimentary rocks, especially if further studies following similar sampling approach can confirm not only existence of particulate Fe and As in fractures but also the transport along the fractures.

Mobilization of As in the tested wells appears to start with oxidation of As-bearing sulfides in the oxic zones of the aquifers and continues in the suboxic zone until oxygen is depleted. This releases As(III) and Fe(II) that in turn is oxidized to hydrous ferric oxide particulates capable of sorbing both As(III) and As(V). These particles are small enough to be transported along the groundwater flow path in fractures before entering the boreholes. Thus

NIH-PA Author Manuscript

NIH-PA Author Manuscript

NIH-PA Author Manuscript

boreholes that intercept those fractures having the longest flow paths and hence a higher likelihood of interacting with As-rich primary minerals in the earlier part of the flow path, are likely to be enriched in As in both dissolved and particulate forms.

Acknowledgements

This research is funded by the U.S. National Institute of Environmental Health Sciences Superfund Research Program 2 P42 ES10349 to Y. Zheng. The work was also supported, in part, by the US Geological Survey (USGS) Toxic Substances Hydrology Program. We thank S. Li of Institute of Geochemistry, Chinese Academy of Sciences, M. Rahman of Queens College, and R. Johnston of Maine Geological Survey for assistance during the field work; Z. Cheng of Brooklyn College for assistance with ICP-MS analysis; K. Clauson of Queens College for XRF analysis; J. Ayotte and Z. Szabo of USGS for helpful discussions; and the three Maine families for access to their private wells and their cooperation throughout the study period. The authors thank Joseph Ayotte of USGS, Stephen Peters of Lehigh University, and an anonymous reviewer for helpful comments that clarified the manuscript. The use of trade, product, or firm names is for descriptive purposes only and does not imply an endorsement by the authors or the U.S. Government. This is LDEO contribution # xxxx.

References

Abernathy CO, Liu YP, Longfellow D, Aposhian HV, Beck B, Fowler B, Goyer R, Menzer R, Rossman T, Thompson C, Waalkes M. Arsenic: Health effects, mechanisms of actions, and research issues. Environ. Health Perspect. 1999; 107:593–597. [PubMed: 10379007]

Ahn JS. Geochemical occurrences of arsenic and fluoride in bedrock groundwater: a case study in Geumsan County, Korea. Environ. Geochem. Health. 2012; 34:43–54. [PubMed: 21818560]

Aloupi M, Angelidis M, Gavriil A, Koulousaris M, Varnavas S. Influence of geology on arsenic concentrations in ground and surface water in central Lesvos, Greece. Environmental Monitoring and Assessment. 2009; 151:383–396. [PubMed: 18437513]

Amirbahman A, Kent DB, Curtis GP, Davis JA. Kinetics of sorption and abiotic oxidation of arsenic(III) by aquifer materials. Geochim. Cosmochim. Acta. 2006; 70:533–547.

Armienta MA, Villasenor G, Rodriguez R, Ongley LK, Mango H. The role of arsenic-bearing rocks in groundwater pollution at Zimapan Valley, Mexico. Environmental Geology. 2001; 40:571–581.

Ayotte JD, Montgomery DL, Flanagan SM, Robinson KW. Arsenic in groundwater in eastern New England: occurrence, controls, and human health implications. Environmental Science & Technology. 2003; 37:2075–2083. [PubMed: 12785510]

Ayotte JD, Nielsen MG, Robinson GR, Moore RB. Relation of Arsenic, Iron, and Manganese in Ground Water to Aquifer Type, Bedrock Lithogeochemistry, and Land Use in the New England Coastal Basins. U.S. Geological Survey, Water-Resources Investigations Report 99-4162. 1999:70.

Ayotte JD, Szabo Z, Focazio MJ, Eberts SM. Effects of human-induced alteration of groundwater flow on concentrations of naturally-occurring trace elements at water-supply wells. Appl. Geochem. 2011; 26:747–762.

Bauer M, Blodau C. Arsenic distribution in the dissolved, colloidal and particulate size fraction of experimental solutions rich in dissolved organic matter and ferric iron. Geochim. Cosmochim. Acta. 2009; 73:529–542.

Boyle DR, Turner RJW, Hall GEM. Anomalous arsenic concentrations in groundwaters of an island community, Bowen Island, British Columbia. Environ. Geochem. Health. 1998; 20:199–212.

Cheng Z, Zheng Y, Mortlock R, van Geen A. Rapid multi-element analysis of groundwater by high-resolution inductively coupled plasma mass spectrometry. Anal. Bioanal. Chem. 2004; 379:512–518. [PubMed: 15098084]

Colman JA. Arsenic and uranium in water from private wells completed in bedrock of east-central Massachusetts—Concentrations, correlations with bedrock units, and estimated probability maps. U.S. Geological Survey Scientific Investigations Report 5013. 2011:113.

Cooper HH, Jacob CE. A generalized graphical method for evaluating formation constants and summarizing well field history. Am. Geophys. Union Trans. 1946; 27:526–534.

Davison W, Seed G. The Kinetics of the oxidation of ferrous iron in synthetic and natural waters. Geochim. Cosmochim. Acta. 1983; 47:67–79.

NIH-PA Author Manuscript NIH-PA Author Manuscript NIH-PA Author Manuscript

Dixit S, Hering JG. Comparison of Arsenic(V) and Arsenic(III) Sorption onto Iron Oxide Minerals: Implications for Arsenic Mobility. Environmental Science & Technology. 2003; 37:4182–4189. [PubMed: 14524451]

Drew LJ, Schuenemeyer JH, Armstrong TR, Sutphin DM. Initial yield to depth relation for water wells drilled into crystalline bedrock - Pinardville quadrangle, New Hampshire. Ground Water. 2001; 39:676–684. [PubMed: 11554245]

Flanagan SV, Marvinney RG, Johnston RA, Yang Q, Zheng Y. Dissemination of well water arsenic results to homeowners in Central Maine: Influences on mitigation behavior and continued risks for exposure. Science of the Total Environment. In press.

Ghosh MM, Yuan JR. Adsorption of inorganic arsenic and organoarsenicals on hydrous oxides. Environ. Prog. 1987; 6:150–157.

Giménez J, Martínez M, de Pablo J, Rovira M, Duro L. Arsenic sorption onto natural hematite, magnetite, and goethite. J. Hazard. Mater. 2007; 141:575–580. [PubMed: 16978766]

Goldberg S. Competitive adsorption of arsenate and arsenite on oxides and clay minerals. Soil Sci. Soc. Am. J. 2002; 66:413–421.

Gotkowitz MB, Schreiber ME, Sim JA. Effects of water use on arsenic release to well water in a confined aquifer. Ground Water. 2004; 42:568–575. [PubMed: 15318779]

Gunnars A, Blomqvist S, Johansson P, Andersson C. Formation of Fe(III) oxyhydroxide colloids in freshwater and brackish seawater, with incorporation of phosphate and calcium. Geochim. Cosmochim. Acta. 2002; 66:745–758.

Guo HM, Zhang B, Zhang Y. Control of organic and iron colloids on arsenic partition and transport in high arsenic groundwaters in the Hetao basin, Inner Mongolia. Appl. Geochem. 2011; 26:360–370.

Hamel SC, Buckley B, Lioy PJ. Bioaccessibility of metals in soils for different liquid to solid ratios in synthetic gastric fluid. Environmental Science & Technology. 1998; 32:358–362.

Harte P, Ayotte J, Hoffman A, Revesz KM, Belaval M, Lamb S, Bohlke JK. Heterogeneous redox conditions, arsenic mobility, and groundwater flow in a fractured-rock aquifer near a waste repository site in New Hampshire, USA. Hydrogeol. J. 2012; 20:1189–1201.

Harte, PT. University of New Hampshire; 1992. Regional ground-water flow in crystalline bedrock and interaction with glacial drift in the New England Uplands; p. 1-147.published Master's thesis

Heinrichs G, Udluft P. Natural arsenic in Triassic rocks: A source of drinking-water contamination in Bavaria, Germany. Hydrogeol. J. 1999; 7:468–476.

Houben GJ. Iron oxide incrustations in wells. Part 1: genesis, mineralogy and geochemistry. Appl. Geochem. 2003; 18:927–939.

Hsieh PA, Shapiro AMK, Barton CC, Haeni FP, Johnson CD, Martin CW, Paillet FL, Winter TC, Wright DL. Methods of characterizing fluid movement and chemical transport in fractured rocks, in Field trip guidebook for the northeastern United States. University of Massachusetts, contribution. 1993; NO. 67:R1–R30.

Hug SJ, Canonica L, Wegelin M, Gechter D, von Gunten U. Solar Oxidation and Removal of Arsenic at Circumneutral pH in Iron Containing Waters. Environmental Science & Technology. 2001; 35:2114–2121. [PubMed: 11393995]

Hug SJ, Leupin O. Iron-Catalyzed Oxidation of Arsenic(III) by Oxygen and by Hydrogen Peroxide: pH-Dependent Formation of Oxidants in the Fenton Reaction. Environmental Science & Technology. 2003; 37:2734–2742. [PubMed: 12854713]

Jambor JL, Dutrizac JE. Occurrence and constitution of natural and synthetic ferrihydrite, a widespread iron oxyhydroxide. Chem. Rev. 1998; 98:2549–2585. [PubMed: 11848971]

James RE, Ferris FG. Evidence for microbial-mediated iron oxidation at a neutrophilic groundwater spring. Chem. Geol. 2004; 212:301–311.

Jang M, Min SH, Kim TH, Park JK. Removal of arsenite and arsenate using hydrous ferric oxide incorporated into naturally occurring porous diatomite. Environmental Science & Technology. 2006; 40:1636–1643. [PubMed: 16568781]

Jessen S, Larsen F, Koch CB, Arvin E. Sorption and desorption of arsenic to ferrihydrite in a sand filter. Environmental Science & Technology. 2005; 39:8045–8051. [PubMed: 16295873]

NIH-PA Author Manuscript NIH-PA Author Manuscript NIH-PA Author Manuscript

Johnson CD, Joesten PK, Mondazzi RA. Borehole-Geophysical and Hydraulic Investigation of the Fracture-Rock Aquifer near the University of Connecticut Landfill, Storrs, Connecticut, 2000 to 2001. USGS water-resources investigations report 03-4125. 2005

Jung HB, Bostick BC, Zheng Y. Field, Experimental, and Modeling Study of Arsenic Partitioning across a Redox Transition in a Bangladesh Aquifer. Environmental Science & Technology. 2012; 46:1388–1395. [PubMed: 22201284]

Karagas MR, Stukel TA, Tosteson TD. Assessment of cancer risk and environmental levels of arsenic in New Hampshire. International Journal of Hygiene and Environmental Health. 2002; 205:85–94. [PubMed: 12018020]

Katsoyiannis IA, Ruettimann T, Hug SJ. pH dependence of Fenton reagent generation and As(III) oxidation and removal by corrosion of zero valent iron in aerated water. Environmental Science & Technology. 2008; 42:7424–7430. [PubMed: 18939581]

Katsoyiannis IA, Zouboulis AI. Biological treatment of Mn(II) and Fe(II) containing groundwater: kinetic considerations and product characterization. Water Res. 2004; 38:1922–1932. [PubMed: 15026247]

Kenny JF, Barber NL, Hutson SS, Linsey KS, Lovelace JK, Maupin MA. Estimated Use of Water in the United States in 2005. U.S. Geological Survey Circular. 2009; 1334

Kim D, Miranda ML, Tootoo J, Bradley P, Gelfand AE. Spatial Modeling for Groundwater Arsenic Levels in North Carolina. Environmental Science & Technology. 2011; 45:4824–4831. [PubMed: 21528844]

Kim M-J, Nriagu J. Oxidation of arsenite in groundwater using ozone and oxygen. Science of The Total Environment. 2000; 247:71–79. [PubMed: 10721144]

Kim MJ, Nriagu J, Haack S. Arsenic behavior in newly drilled wells. Chemosphere. 2003; 52:623–633. [PubMed: 12738300]

Ko I, Kim JY, Kim KW. Arsenic speciation and sorption kinetics in the As35 hematite-humic acid system. Colloid Surf. A-Physicochem. Eng. Asp. 2004; 234:43–50.

Kortatsi B. Hydrochemical framework of groundwater in the Ankobra Basin, Ghana. Aquatic Geochemistry. 2007; 13:41–74.

Lane JW Jr, Williams JH, Johnson CD, Savino DM, Haeni FP. An Integrated Geophysical and Hydraulic Investigation to Characterize a Fractured-Rock Aquifer, Norwalk, Connecticut, USGS Water-Resources Investigation Report 01-4133. 2002

Lenoble V, Bouras O, Deluchat V, Serpaud B, Bollinger J-C. Arsenic Adsorption onto Pillared Clays and Iron Oxides. J. Colloid Interface Sci. 2002; 255:52–58. [PubMed: 12702367]

Lin Z, Puls RW. Adsorption, desorption and oxidation of arsenic affected by clay minerals and aging process. Environmental Geology. 2000; 39:753–759.

Lipfert G, Reeve AS, Sidle WC, Marvinney R. Geochemical patterns of arsenic-enriched ground water in fractured, crystalline bedrock, Northport, Maine, USA. Appl. Geochem. 2006; 21:528–545.

Lipfert G, Sidle WC, Reeve AS, Ayuso RA, Boyce AJ. High arsenic concentrations and enriched sulfur and oxygen isotopes in a fractured-bedrock ground-water system. Chem. Geol. 2007; 242:385–399.

Liu GL, Fernandez A, Cai Y. Complexation of Arsenite with Humic Acid in the Presence of Ferric Iron. Environmental Science & Technology. 2011; 45:3210–3216. [PubMed: 21322632]

Mack, TJ.; Belaval, M.; Degnan, JR.; Roy, SJ.; Ayotte, JD. Geophysical and flow-weighted natural-contaminant characterization of three water-supply wells in New Hampshire: U.S. Geological Survey Open-File Report 2011–1019; 2011. p. 20at http://pubs.usgs.gov/of/2011/1019/.

Mahler RL, Simmons R, Sorensen F. Public perceptions and actions towards sustainable groundwater management in the pacific northwest region, USA. Int. J. Water Resour. Dev. 2005; 21:465–472.

Meng X, Bang S, Korfiatis GP. Effects of silicate, sulfate, and carbonate on arsenic removal by ferric chloride. Water Res. 2000; 34:1255–1261.

Nielsen, MG.; Lombard, PJ.; Schalk, LF. Assessment of Arsenic Concentrations in Domestic Well Water, by Town, in Maine, 2005–09 U.S. Geological Survey Scientific Investigations Report 2010–5199; 2010. p. 68(Also available at http://pubs.usgs.gov/sir/2010/5199.).

Nordstrom DK, Olsson T, Carlsson L, Fritz P. Introduction to the hydrogeochemical investigations within the International Stripa Project. Geochim. Cosmochim. Acta. 1989; 53:1717–1726.

NIH-PA Author Manuscript NIH-PA Author Manuscript NIH-PA Author Manuscript

Paillet FL. Flow modeling and permeability estimation using borehole flow logs in heterogeneous fractured formations. Water Resour. Res. 1998; 34:997–1010.

Paillet FL, Kapucu K. Fracture characterization and fracture-permeability estimates from geophysical logs in the Mirror Lake Watershed, New Hampshire. U.S. Geological Survey, Water-Resources Investigations Report 89-4058. 1989

Pedrot M, Le Boudec A, Davranche M, Dia A, Henin O. How does organic matter constrain the nature, size and availability of Fe nanoparticles for biological reduction? J. Colloid Interface Sci. 2011; 359:75–85. [PubMed: 21482426]

Peters SC. Arsenic in groundwaters in the Northern Appalachian Mountain belt: A review of patterns and processes. J. Contam. Hydrol. 2008; 99:8–21. [PubMed: 18571283]

Peters SC, Blum JD. The source and transport of arsenic in a bedrock aquifer, New Hampshire, USA. Appl. Geochem. 2003; 18:1773–1787.

Peters SC, Burkert L. The occurrence and geochemistry of arsenic in groundwaters of the Newark basin of Pennsylvania. Appl. Geochem. 2008; 23:85–98.

Pierce ML, Moore CB. Adsorption of arsenite and arsenate on amorphous iron hydroxide. Water Res. 1982; 16:1247–1253.

Pippin, CG.; Reid, JC.; Withers, C.; Ennism, L. Abstract in The 231st ACS National Meeting. Atlanta, GA: 2006. Generalized geochemical model for arsenic fate and transport in the unconfined fractured bedrock aquifer system of the North Carolina piedmont. 2006

Pullin MJ, Cabaniss SE. The effects of pH, ionic strength, and iron-fulvic acid interactions on the kinetics of nonphotochemical iron transformations. I. Iron(II) oxidation and iron(III) colloid formation. Geochim. Cosmochim. Acta. 2003; 67:4067–4077.

Radloff KA, Zheng Y, Michael HA, Stute M, Bostick BC, Mihajlov I, Bounds M, Huq MR, Choudhury I, Rahman MW, Schlosser P, Ahmed KM, van Geen A. Arsenic migration to deep groundwater in Bangladesh influenced by adsorption and water demand. Nat. Geosci. 2011; 4:793–798. [PubMed: 22308168]

Raven KP, Jain A, Loeppert RH. Arsenite and arsenate adsorption on ferrihydrite: Kinetics, equilibrium, and adsorption envelopes. Environmental Science & Technology. 1998; 32:344–349.

Rice DC, Lincoln R, Martha J, Parker L, Pote K, Xing SQ, Smith AE. Concentration of metals in blood of Maine children 1–6 years old. Journal of Exposure Science and Environmental Epidemiology. 2012; 20:634–643. [PubMed: 20664650]

Ryan PC, Kim J, Wall AJ, Moen JC, Corenthal LG, Chow DR, Sullivan CM, Bright KS. Ultramafic-derived arsenic in a fractured bedrock aquifer. Appl. Geochem. 2011; 26:444–457.

Shapiro AM. Effective matrix diffusion in kilometer-scale transport in fractured crystalline rock. Water Resour. Res. 2001; 37:507–522.

Shapiro AM. Cautions and suggestions for geochemical sampling in fractured rock. Ground Water Monitoring and Remediation. 2002; 22:151–164.

Shukla DP, Dubey CS, Singh NP, Tajbakhsh M, Chaudhry M. Sources and controls of Arsenic contamination in groundwater of Rajnandgaon and Kanker District, Chattisgarh Central India. Journal of Hydrology. 2010; 395:49–66.

Sidle W. 18OSO4 and 18OH2O as prospective indicators of elevated arsenic in the Goose River ground-watershed, Maine. Environmental Geology. 2002; 42:350–359.

Sidle WC. Identifying discharge zones of arsenic in the Goose River Basin, Maine. J. Am. Water Resour. Assoc. 2003; 39:1067–1077.

Sidle WC, Fischer RA. Detection of H-3 and Kr-85 in groundwater from arsenic-bearing crystalline bedrock of the Goose River basin, Maine. Environmental Geology. 2003; 44:781–789.

Sidle WC, Wotten B, Murphy E. Provenance of geogenic arsenic in the Goose River basin, Maine, USA. Environmental Geology. 2001; 41:62–73.

Smedley PL. Arsenic in rural groundwater in Ghana. Journal of African Earth Sciences. 1996; 22:459–470.

Smedley PL, Knudsen J, Maiga D. Arsenic in groundwater from mineralised Proterozoic basement rocks of Burkina Faso. Appl. Geochem. 2007; 22:1074–1092.

NIH-PA Author Manuscript

NIH-PA Author Manuscript

NIH-PA Author Manuscript

Stolpe B, Guo L, Shiller AM, Aiken GR. Abundance, size distributions and trace-element binding of organic and iron-rich nanocolloids in Alaskan rivers, as revealed by field-flow fractionation and ICP-MS. Geochim. Cosmochim. Acta. 2013; 105:221–239.

Thompson A, Chadwick OA, Boman S, Chorover J. Colloid mobilization during soil iron redox oscillations. Environmental Science & Technology. 2006; 40:5743–5749. [PubMed: 17007135]

Utsunomiya S, Peters SC, Blum JD, Ewing RC. Nanoscale mineralogy of arsenic in a region of New Hampshire with elevated As-concentrations in the groundwater. Am. Mineral. 2003; 88:1844–1852.

Wilkie JA, Hering JG. Rapid Oxidation of Geothermal Arsenic(III) in Streamwaters of the Eastern Sierra Nevada. Environmental Science & Technology. 1998; 32:657–662.

Wolthoorn A, Temminghoff EJM, van Riemsdijk WH. Colloid formation in groundwater by subsurface aeration: characterisation of the geo-colloids and their counterparts. Appl. Geochem. 2004; 19:1391–1402.

Yang Q, Jung H-B, Culbertson CW, Marvinney RG, Zheng Y. Can arsenic occurrence rates in bedrock aquifers be predicted? Environmental Science & Technology. 2012; 46:2080–2087. [PubMed: 22260208]

Yang Q, Jung HB, Culbertson CW, Marvinney RG, Loiselle MC, Locke DB, Cheek H, Thibodeau H, Zheng Y. Spatial Pattern of Groundwater Arsenic Occurrence and Association with Bedrock Geology in Greater Augusta, Maine. Environmental Science & Technology. 2009; 43:2714–2719. [PubMed: 19475939]

NIH-PA Author Manuscript

NIH-PA Author Manuscript

NIH-PA Author Manuscript

Highlights

- Most Fe and some As exist in particulate in the tested borehole and fracture water.
- Oxidation of As-containing sulfides results in a reservoir of As-rich Fe-particles.
- Re-mobilization of As from particles is possible in anoxic zones of the aquifer.
- A conceptual model illustrates the role of flow and sorption controls on As.

NIH-PA Author Manuscript

NIH-PA Author Manuscript

NIH-PA Author Manuscript

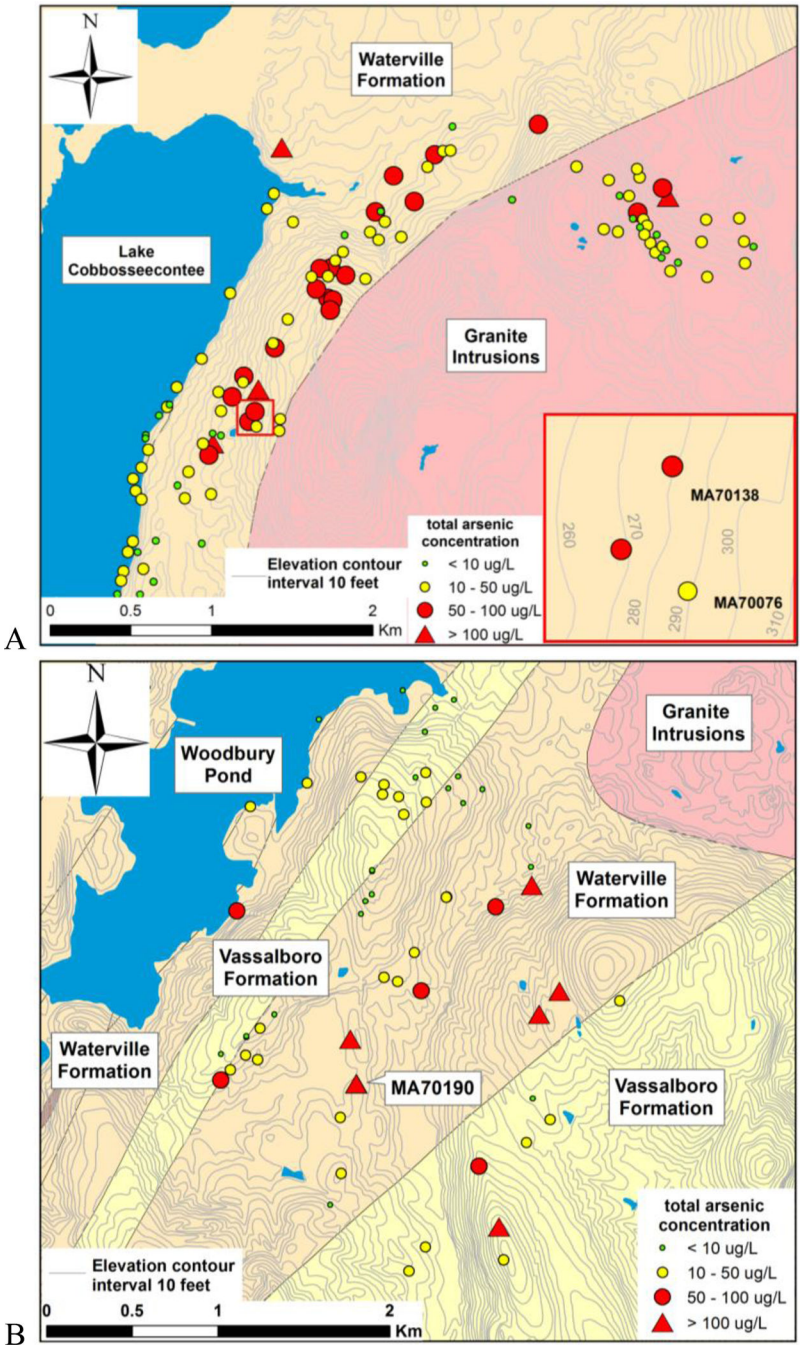

Figure 1.

Total arsenic concentrations in groundwater plotted on bedrock geology (source: Maine Geological Survey) and topographic maps at Manchester (A) and Litchfield (B), central Maine

NIH-PA Author Manuscript

NIH-PA Author Manuscript

NIH-PA Author Manuscript

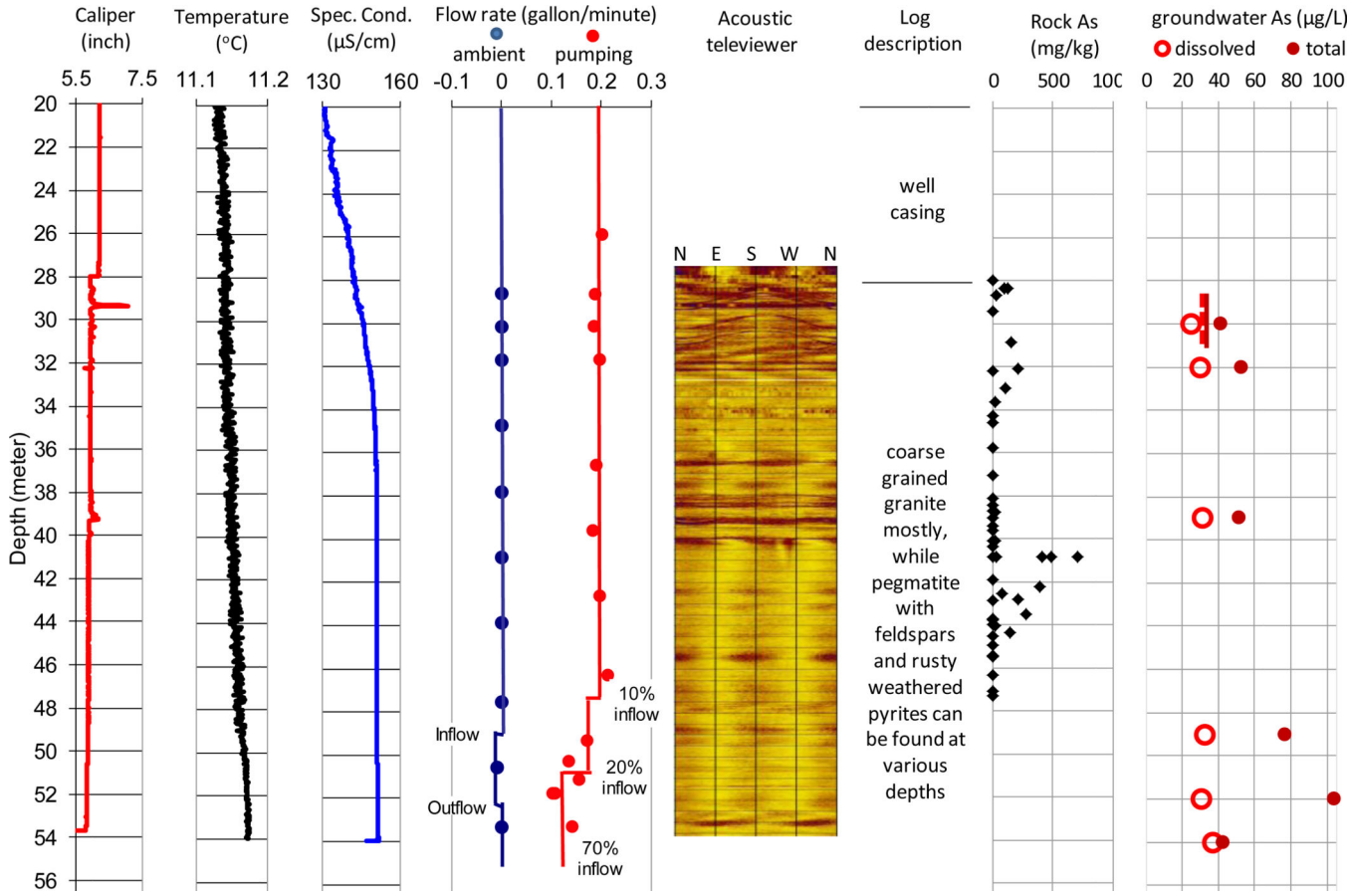

Figure 2.

Composite logs of caliper, water temperature, specific conductance, heat-pulse flow meter, acoustic televiewer, core description, rock arsenic concentrations, and fracture water dissolved arsenic concentrations in well MA70076 in Manchester, Maine

* Groundwater [As] at the end of pumping test: dash line – dissolved [As], solid line – total [As].

NIH-PA Author Manuscript

NIH-PA Author Manuscript

NIH-PA Author Manuscript

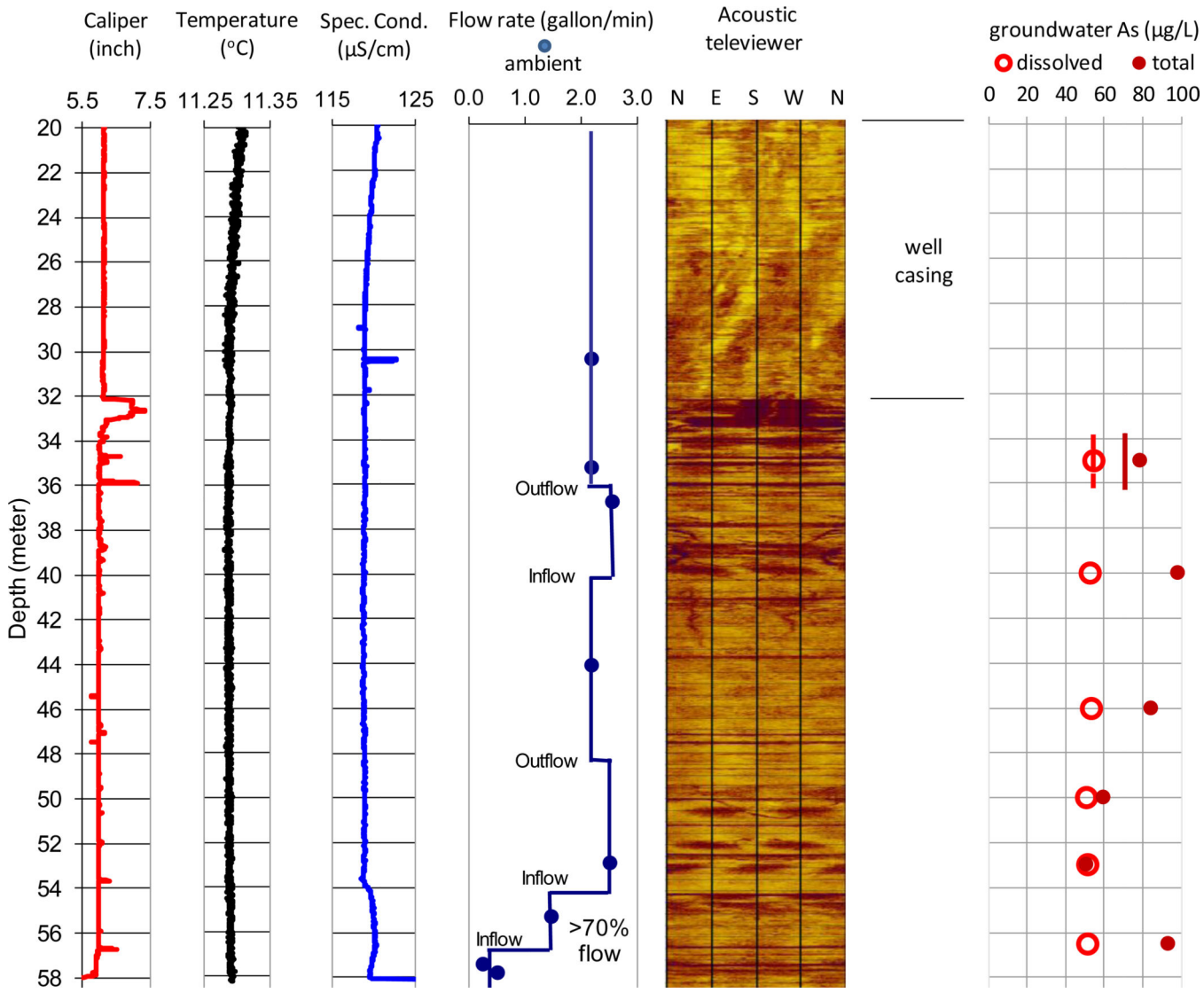

Figure 3.

Composite logs of caliper, water temperature, specific conductance, heat-pulse flow meter, acoustic televiewer, and fracture water dissolved arsenic concentrations in well MA70138 in Manchester, Maine

* Groundwater [As] at the end of pumping test: dash line – dissolved [As], solid line – total [As].

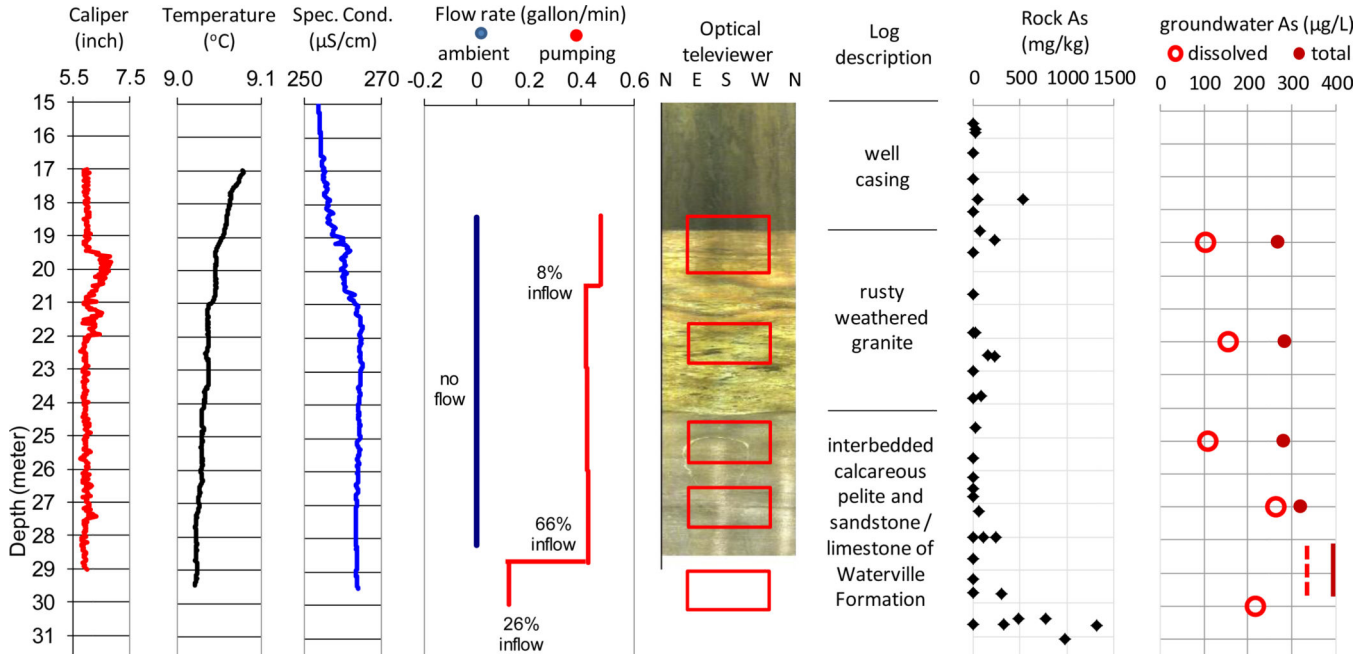

Figure 4.

Composite logs of caliper, water temperature, specific conductance, heat-pulse flow meter, optical televiewer, core description, rock arsenic concentrations, and fracture water dissolved arsenic concentrations in well MA70190 in Litchfield, Maine

* Red squares indicate the sampling intervals for fracture specific water.

* Groundwater [As] at the end of pumping test: dash line – dissolved [As], solid line – total [As].

NIH-PA Author Manuscript NIH-PA Author Manuscript NIH-PA Author Manuscript

NIH-PA Author Manuscript

NIH-PA Author Manuscript

NIH-PA Author Manuscript

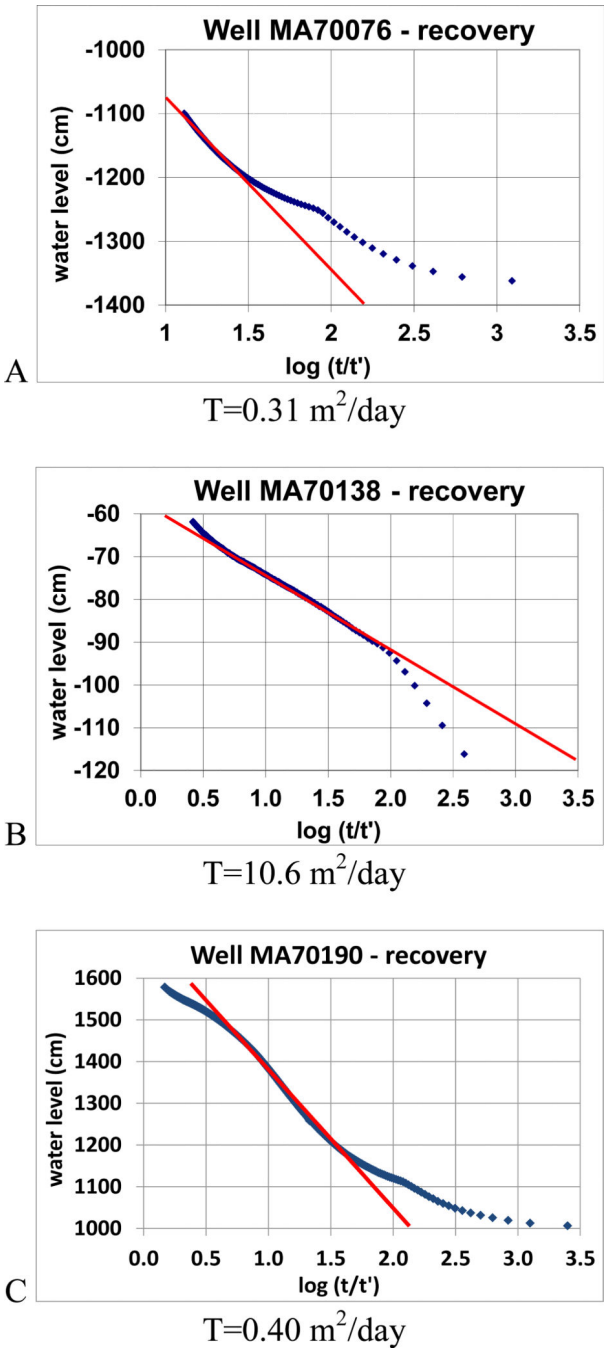

Figure 5.

Cooper-Jacob straight-line method to estimate borehole transmissivity of wells MA70076 (A), MA70138 (B), and MA70190 (C)

NIH-PA Author Manuscript
NIH-PA Author Manuscript
NIH-PA Author Manuscript

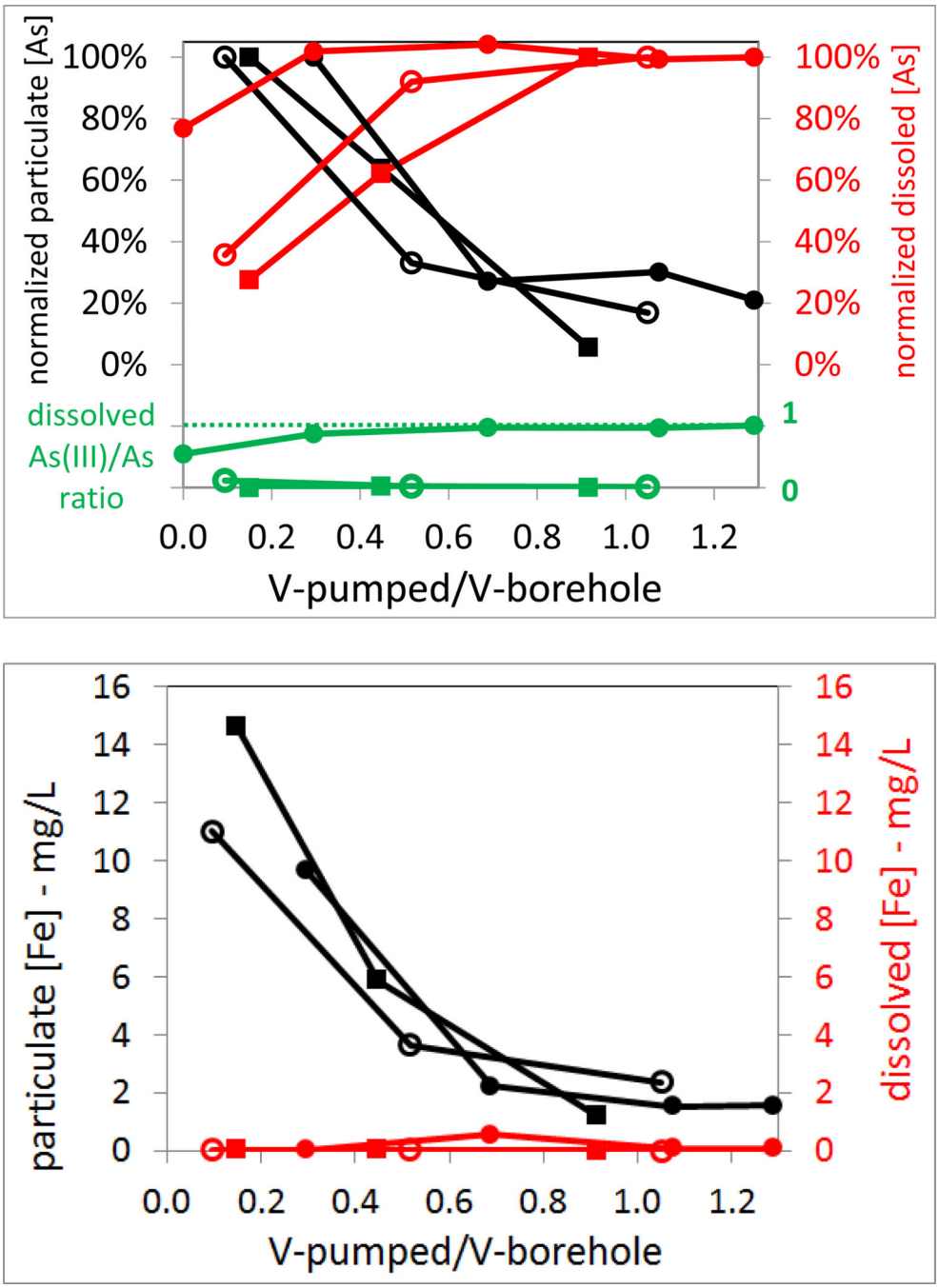

Figure 6.

Borehole water arsenic (normalized to the maximum concentrations) and dissolved As(III)/As ratio (top), and iron concentrations (bottom) during pumping tests in wells MA70076 (solid square), MA70138 (open circle), and MA70190 (solid circle)

NIH-PA Author Manuscript
NIH-PA Author Manuscript
NIH-PA Author Manuscript

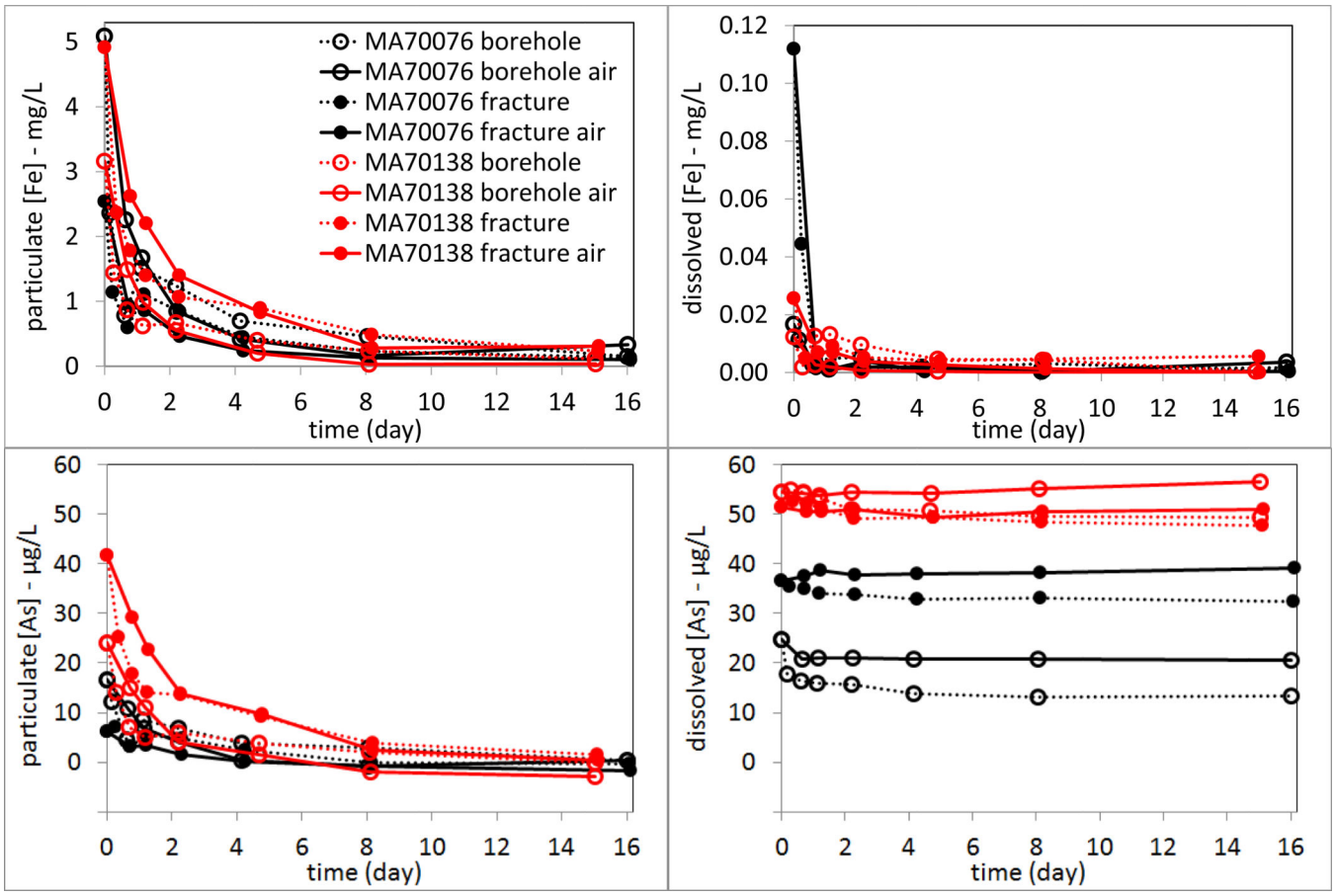

Figure 7.
Arsenic and iron concentrations in cubitainer experiments

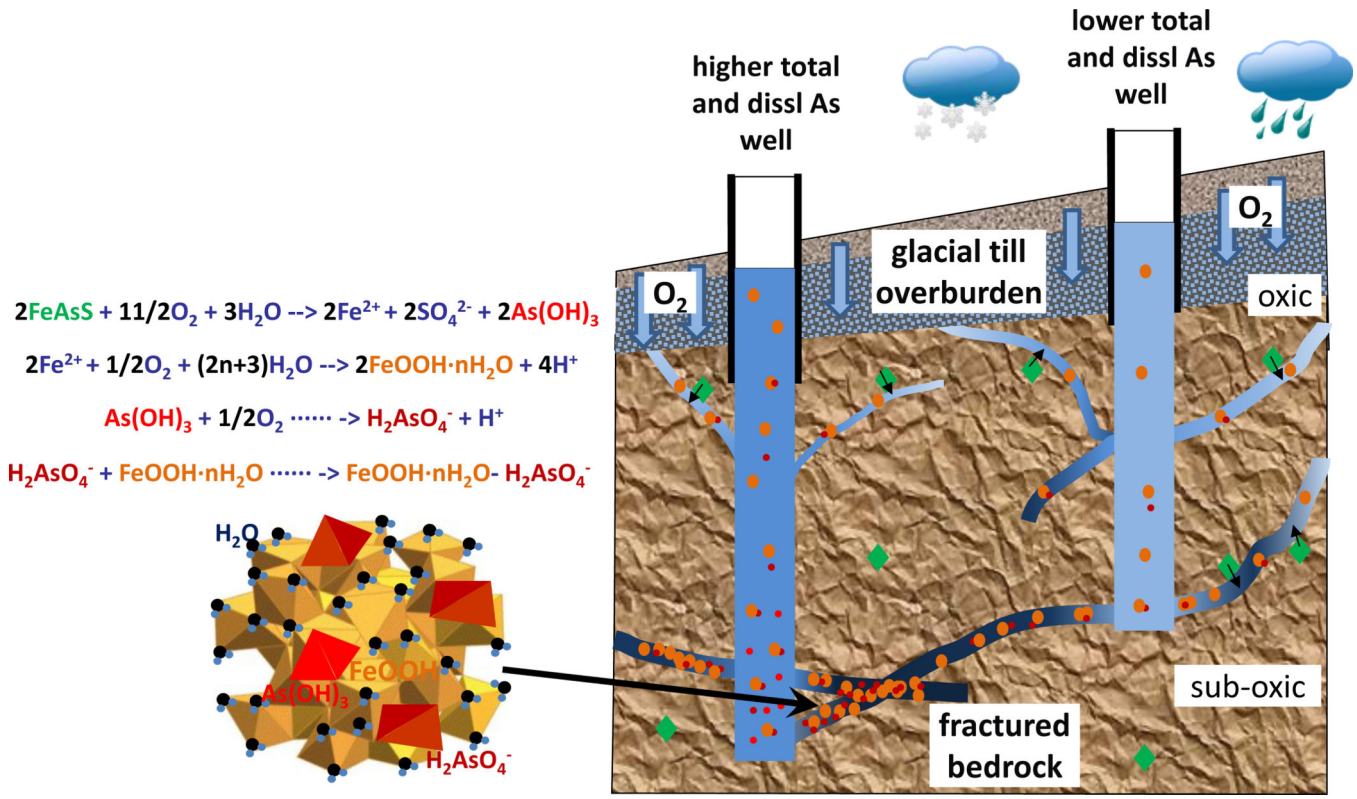

Figure 8.

A schematic graph (right) and geochemical processes (left) of arsenic evolution along groundwater flow paths in fractured bedrock aquifers in central Maine

* The intensity of blue colors reflects the redox conditions, with light blue indicating more oxic and dark blue more sub-oxic.

NIH-PA Author Manuscript NIH-PA Author Manuscript NIH-PA Author Manuscript

NIH-PA Author Manuscript

NIH-PA Author Manuscript

NIH-PA Author Manuscript

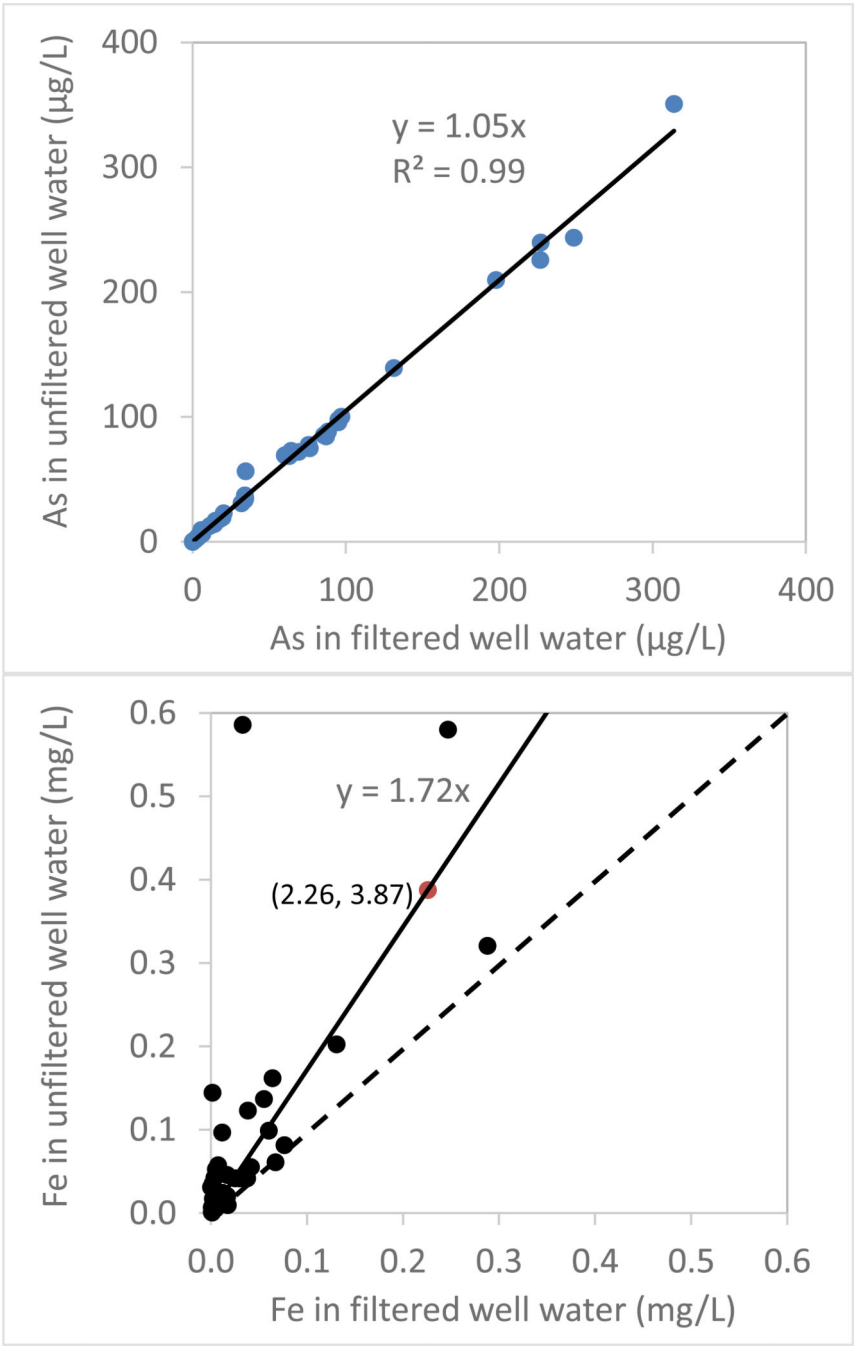

Figure 9.

Arsenic concentrations in µg/L (top) and iron concentrations in mg/L (bottom) in unfiltered and filtered (0.45-µm) water samples from 25 private bedrock wells in central Maine

* Dashed line indicates 1:1 ratio.

NIH-PA Author Manuscript
NIH-PA Author Manuscript
NIH-PA Author Manuscript

Table 1

Pumping and sampling history, geochemistry of groundwater samples in well MA70076

year	pumping time (min)	pumping rate (L/min)	pumped / borehole volume	sample ID	sampling depth (m)	pH	DO (mg/L)	Spec. Cond. (μS/cm)	total [As] (μg/L)	dissolved [As] (μg/L)	dissolved As(III) (μg/L)	dissolved As(III)/As ratio	total [Fe] (μg/L)	dissolved [Fe] (μg/L)	particulate As/Fe (mmol/mol)	estimated particulate As (mg/kg)	Xd (adsorb. As/diss. As) (L/kg)
2007	15	from hose		MA70076	hose	7.50	3.0	ND	38	ND	ND	ND	2,190	ND	ND	ND	ND
2008	0	15.9															
	30	15.9	0.55	P70076.0	30.5	7.80	4.1	128	20	14.1	ND	ND	155,000	563	0.03	9	6E+02
	113	15.9	2.08	P70076.1	52	7.85	3.9	126	ND	24.1	2.3	10%	9,740	232	ND	ND	ND
2009	0	3.7															
	35	3.7	0.15	B70076.1	30	7.17	8.7	240	67	7.7	0.0	0%	14,600	22	3	940	1E+05
	105	3.7	0.45	B70076.2	30	7.12	5.4	226	55	17.4	0.5	3%	5,910	28	5	1500	9E+04
	215	3.7	0.92	B70076.3	30	7.06	4.0	191	31	28.0	0.1	0%	1,220	7	2	640	2E+04
		3.6		F70076.1	54	7.22	5.0	252	43	36.7	0.3	1%	2,650	112	2	560	2E+04
		2.9		F70076.2	52	7.21	5.0	251	104	30.4	0.1	0%	23,400	19	2	720	2E+04
		2.7		F70076.3	49	7.18	5.0	243	77	32.5	0.6	2%	11,000	18	3	930	3E+04
		2.7		F70076.4	39	7.21	4.0	236	52	31.3	0.4	1%	5,850	11	3	810	3E+04
		2.8		F70076.5	32	7.20	4.0	237	53	29.8	0.5	2%	6,620	24	3	800	3E+04
		2.6		F70076.6	30	7.22	4.0	251	41	24.7	0.8	3%	5,100	17	2	760	3E+04

year	sample ID	Cl^- (mg/L)	SO_4^{2-} (mg/L)	alkalinity (mmol/L)	Na (mg/L)	Mg (mg/L)	K (mg/L)	Ca (mg/L)	Σ major ion (meq/L)
2007	MA70076	1.7	7.1	1.1	5.6	1.5	1.1	17.3	1.3
2008									
	P70076.0	1.4	6.6	1.1	4.9	1.2	0.8	22.3	1.4
	P70076.1	1.4	6.5	1.2	5.6	1.2	0.9	21.7	1.4
2009									
	B70076.1	1.6	6.1	ND	ND	ND	ND	ND	ND
	B70076.2	1.5	6.6	ND	5.2	1.8	0.9	22.8	1.5
	B70076.3	1.5	6.9	ND	5.3	1.9	1.0	25.2	1.7
	F70076.1	1.5	7.0	ND	4.6	1.7	0.8	22.5	1.5
	F70076.2	1.5	7.1	ND	4.3	1.6	0.8	20.9	1.4
	F70076.3	1.5	6.9	ND	4.6	1.7	0.8	22.2	1.5

Sci Total Environ. Author manuscript; available in PMC 2016 February 01.

NIH-PA Author Manuscript
NIH-PA Author Manuscript
NIH-PA Author Manuscript

year	sample ID	Cl^- (mg/L)	SO_4^{2-} (mg/L)	alkalinity (mmol/L)	Na (mg/L)	Mg (mg/L)	K (mg/L)	Ca (mg/L)	Σ major ion (meq/L)
	F70076.4	1.7	6.8	1.0	4.8	1.7	0.8	22.2	1.3
	F70076.5	1.5	6.9	1.1	ND	ND	ND	ND	1.3
	F70076.6	1.5	6.9	1.2	5.0	1.8	0.9	23.5	1.5

*ND – no data

*Sum of major ions is calculated based on major anions (Cl^-, SO_4^{2-}, HCO_3^-), or major cations (Na, Mg, K, Ca), or the average of the sum of major anions and the sum of major cations if both are available.

NIH-PA Author Manuscript NIH-PA Author Manuscript NIH-PA Author Manuscript

Table 2

Pumping and sampling history, geochemistry of groundwater samples in well MA70138

year	pumping time (min)	pumping rate (L/min)	pumped / borehole volume	sample ID	sampling depth (m)	pH	DO (mg/L)	Spec. Cond. (μS/cm)	total [As] (μg/L)	dissolved [As] (μg/L)	dissolved As(III) (μg/L)	dissolved As(III)/As ratio	total [Fe] (μg/L)	dissolved [Fe] (μg/L)	particulate As/Fe (mmol/mol)	estimated particulate As (mg/kg)	Xd (adsorb. As/diss. As) (L/kg)
2007	15	from hose		MA70138	hose	8.18	1.0	ND	73	ND	ND	ND	50	ND	ND	ND	ND
2008	0	7.9															
	60	7.9	0.45	P70138.0	0	7.91	5.2	144	649	10.0	ND	ND	175,000	1390	3	850	8E+04
	470	31.0	3.37	P70138.1	57	8.03	0.7	142	117	21.0	4.2	20%	26,200	564	3	860	4E+04
	550	31.0	5.73	P70138.2	52	7.93	2.2	142	47	46.2	5.3	11%	3,180	67	0.3	90	2E+03
2009	0	9.1															
	11	9.1	0.09	B70138.1	35	7.46	2.0	149	119	19.4	2.2	11%	11,000	40	7	2100	1E+05
	60	9.1	0.52	B70138.2	35	7.49	3.0	145	83	50.0	1.0	2%	3,680	36	7	2100	4E+04
	122	9.1	1.05	B70138.3	35	7.54	3.0	145	71	54.3	0.7	1%	2,380	10	5	1600	3E+04
		5.3		F70138.1	56.5	7.72	1.0	147	93	51.5	0.5	1%	4,940	26	6	1900	4E+04
		5.3		F70138.2	53	7.71	2.0	145	51	51.7	0.0	0%	870	4	ND	ND	ND
		5.3		F70138.3	50	7.56	1.0	142	60	50.7	0.6	1%	1,300	11	5	1600	3E+04
		5.3		F70138.4	46	7.43	1.0	143	84	53.1	0.0	0%	4,300	15	5	1700	3E+04
		5.3		F70138.5	40	7.74	1.0	145	98	52.5	0.1	0%	4,440	15	8	2400	5E+04
		5.3		F70138.6	35	7.75	2.0	144	79	54.4	0.6	1%	3,170	12	6	1800	3E+04

year	sample ID	Cl^- (mg/L)	SO_4^{2-} (mg/L)	alkalinity (mmol/L)	Na (mg/L)	Mg (mg/L)	K (mg/L)	Ca (mg/L)	Σ major ion (meq/L)
2007	MA70138	1.1	5.8	1.1	5.6	0.4	0.6	24.5	1.4
2008									
	P70138.0	1.1	6.4	1.1	7.3	1.3	1.0	23.1	1.4
	P70138.1	1.3	5.8	1.3	7.3	1.3	1.0	24.7	1.6
	P70138.2	1.1	5.5	1.4	8.5	1.3	1.1	24.7	1.6
2009									
	B70138.1	1.1	5.7	1.3	ND	ND	ND	ND	1.5
	B70138.2	1.3	5.7	1.3	ND	ND	ND	ND	1.5
	B70138.3	1.1	5.8	1.4	ND	ND	ND	ND	1.5
	F70138.1	1.1	5.6	1.3	6.1	1.5	0.7	19.5	1.4

Sci Total Environ. Author manuscript; available in PMC 2016 February 01.

NIH-PA Author Manuscript
NIH-PA Author Manuscript
NIH-PA Author Manuscript

year	sample ID	Cl^- (mg/L)	SO_4^{2-} (mg/L)	alkalinity (mmol/L)	Na (mg/L)	Mg (mg/L)	K (mg/L)	Ca (mg/L)	Σ major ion (meq/L)
	F70138.2	1.2	5.6	1.3	5.3	1.4	0.7	18.7	1.4
	F70138.3	1.1	5.8	1.3	4.8	1.3	0.6	17.1	1.3
	F70138.4	1.2	5.7	1.3	4.1	1.1	0.4	15.3	1.2
	F70138.5	1.2	5.8	1.3	4.1	1.1	0.4	15.1	1.2
	F70138.6	1.2	5.8	ND	6.0	1.6	0.8	21.9	1.5

*ND – no data

*Sum of major ions is calculated based on major anions (Cl^-, SO_4^{2-}, HCO_3^-), or major cations (Na, Mg, K, Ca), or the average of the sum of major anions and the sum of major cations if both are available.

NIH-PA Author Manuscript NIH-PA Author Manuscript NIH-PA Author Manuscript

Table 3

Pumping and sampling history, geochemistry of groundwater samples in well MA70190

year	pumping time (min)	pumping rate (L/min)	pumped / borehole volume	pumped / packed volume	sample ID	sampling depth (m)	pH	DO (mg/L)	Spec. Cond. (μS/cm)	total [As] (μg/L)	dissolved [As] (μg/L)	dissolved [As] (III) (μg/L)	dissolved As(III)/As ratio	total [Fe] (μg/L)	dissolved [Fe] (μg/L)	particulate As/Fe (mmol/mol)	estimated particulate As (mg/kg)	Xd (asorb. As/diss. As) (L/kg)
2007	15	from hose			MA70190	hose	8.17	0.6	ND	478	ND	ND	ND	7420	ND	ND	ND	ND
2010	0	5.3			B70190.0	24.4	ND	ND	ND	8180	257	140	55%	415000	260	14	4400	2E+04
	48	5.3	0.30		B70190.1	29	7.84	5.2	233	621	340	298	88%	9730	36	22	6700	2E+04
	112	5.3	0.69		B70190.2	29	7.96	3.4	233	424	348	341	98%	2800	574	25	7900	2E+04
	175	5.3	1.08		B70190.3	29	7.98	1.2	232	417	332	323	97%	1640	103	41	13000	4E+04
	210	5.3	1.29		B70190.4	29	7.98	0.7	230	393	334	338	100%	1670	91	28	8600	3E+04
		2.3		3.9	F70190.1	>29	7.87	4.5	247	2560	217	247	110%	80400	142	22	6700	3E+04
		1.5		1.9	F70190.2	27	7.88	8.2	255	321	262	269	100%	4430	675	12	3600	1E+04
		0.8		1.4	F70190.3	25	7.59	9.9	263	280	109	107	98%	5370	20	24	7300	7E+04
		2.3		2.6	F70190.4	22	7.59	5.5	265	283	155	136	88%	4940	185	20	6200	4E+04
		2.3		6.9	F70190.5	<20	7.59	7.6	263	269	103	90	87%	6340	199	20	6200	6E+04

year	sample ID	$\delta^{18}O$ ‰	$\delta^{2}H$ ‰	Cl^- (mg/L)	SO_4^{2-} (mg/L)	alkalinity (mmol/L)	Na (mg/L)	Mg (mg/l)	K (mg/L)	Ca (mg/L)	Σ major ion (meq/L)
2007	MA70190	ND	ND	29.9	13.3	1.0	5.9	1.7	2.1	26.9	1.9
2010	B70190.0	−9.71	−63.3	31.2	14.5	ND	7.8	4.0	2.5	30.7	2.3
	B70190.1	−9.68	−62.4	25.1	16.0	1.0	9.0	4.3	2.6	29.9	2.2
	B70190.2	−9.64	−63.4	26.1	16.8	ND	7.1	4.1	2.5	25.2	2.0
	B70190.3	−9.66	−63.3	25.6	16.5	1.0	7.0	2.5	1.9	23.2	1.9
	B70190.4	−9.74	−63.5	25.8	16.9	ND	7.1	4.1	3.1	27.8	2.1
	F70190.1	−9.82	−63.8	30.2	16.1	ND	6.8	4.3	2.8	25.6	2.0
	F70190.2	−9.70	−64.1	35.3	13.8	ND	7.2	4.2	2.4	31.1	2.3
	F70190.3	−9.71	−64.2	38.4	13.5	ND	7.5	4.6	2.7	40.9	2.8
	F70190.4	−9.72	−64.5	39.7	12.8	ND	6.6	4.8	2.8	34.2	2.5
	F70190.5	−9.73	−64.2	37.6	13.1	ND	7.3	4.5	3.4	34.3	2.5

*ND – no data

*The over 100% dissolved As(III)/As ratio might be caused by the analytical error and dilution effects during sample preparation.

NIH-PA Author Manuscript

NIH-PA Author Manuscript

NIH-PA Author Manuscript

* Sum of major ions is calculated based on major anions (Cl^-, SO_4^{2-}, HCO_3^-), or major cations (Na, Mg, K, Ca), or the average of the sum of major anions and the sum of major cations if both are available.

NIH-PA Author Manuscript

NIH-PA Author Manuscript

NIH-PA Author Manuscript

Table 4

Arsenic, iron concentrations, and arsenic partitioning ratios in cubitainer experiments

Sample	Time	pH	Iron (Fe)		Arsenic (As)			particulate	As partitioning Xd
			total	dissolved	total	dissolved	diss.As(III)	As/Fe	adsorb.As/diss. As
	day		µg/L	µg/L	µg/L	µg/L	µg/	mmol/mol	L/kg
MA70076 bore hole water	0	7.22	5100	16.6	41.4	24.7	0.8	2	3E+04
	0.2	ND	2370	11.3	30.0	17.7	0.1	4	7E+04
	0.6	7.25	780	2.6	21.0	16.5	0.1	4	8E+04
	1.1	7.91	1510	4.8	24.4	15.8	0.1	4	8E+04
	2.2	7.34	1240	5.3	22.7	15.7	0.1	4	8E+04
	4.2	7.58	700	1.9	17.7	13.9	0.1	4	9E+04
	8.0	7.52	460	1.0	16.0	13.1	0.0	5	1E+05
	16.0	7.78	150	1.7	13.7	13.4	0.2	1	3E+04
MA70076 bore hole water with air purging	0	7.22	5100	16.6	41.4	24.7	0.8	2	3E+04
	0.6	7.67	2260	2.5	31.6	20.8	0.2	4	5E+04
	1.1	7.98	1670	1.2	28.0	21.1	0.1	3	5E+04
	2.2	7.87	850	1.9	25.1	21.0	0.5	4	5E+04
	4.2	7.70	420	1.8	21.2	20.8	0.2	1	1E+04
	8.1	7.61	160	0.4	20.0	20.8	0.3	NA	NA
	16.0	8.19	340	3.6	21.0	20.5	0.4	1	1E+04
MA70076 fracture water	0	7.22	2650	112.0	42.8	36.7	0.3	2	2E+04
	0.2	ND	1190	44.4	42.4	35.3	0.1	5	4E+04
	0.7	7.53	600	3.5	38.2	35.0	0.1	4	4E+04
	1.2	7.53	1110	2.0	39.5	34.1	0.1	4	3E+04
	2.3	7.57	850	1.9	38.4	33.7	0.3	4	4E+04
	4.2	7.59	450	1.4	35.4	32.8	0.6	4	4E+04
	8.1	7.46	230	3.0	32.8	33.0	0.1	NA	NA
	16.1	7.82	130	0.7	32.1	32.5	<DL	NA	NA
MA70076 fracture water with air purging	0	7.22	2650	112.0	42.8	36.7	0.3	2	2E+04
	0.7	7.72	940	1.3	40.8	37.6	0.1	3	2E+04
	1.2	8.02	860	1.2	42.2	38.7	0.1	3	2E+04
	2.3	7.87	470	3.8	39.4	37.8	0.9	3	2E+04
	4.3	7.73	240	0.3	38.2	38.0	1.0	1	5E+03
	8.1	7.89	130	0.4	37.5	38.3	1.3	NA	NA
	16.1	8.23	100	0.3	37.4	39.1	1.2	NA	NA
MA70138 bore hole water	0	7.75	3170	12.3	78.5	54.4	0.6	6	3E+04
	0.3	7.76	1440	1.9	68.9	54.9	0.6	7	4E+04
	0.7	8.23	880	12.6	61.5	54.4	1.4	6	3E+04
	1.2	8.63	630	13.1	58.3	53.3	0.5	6	4E+04
	2.2	8.36	680	9.5	56.8	50.9	0.5	7	4E+04

NIH-PA Author Manuscript

NIH-PA Author Manuscript

NIH-PA Author Manuscript

Sample	Time	pH	Iron (Fe)		Arsenic (As)			particulate	As partitioning Xd
			total	dissolved	total	dissolved	diss.As(III)	As/Fe	adsorb.As/diss. As
	day		µg/L	µg/L	µg/L	µg/L	µg/	mmol/mol	L/kg
	4.7	8.38	400	4.6	54.4	50.6	0.2	7	4E+04
	8.1	8.16	240	4.3	51.7	49.7	0.8	7	4E+04
	15.0	8.12	110	0.4	49.2	49.4	0.1	NA	NA
MA70138 bore hole water with air purging	0	7.75	3170	12.3	78.5	54.4	0.6	6	3E+04
	0.7	7.85	1490	2.6	69.3	54.3	0.5	8	4E+04
	1.2	7.85	980	1.9	64.9	53.8	0.9	8	5E+04
	2.2	7.87	550	0.7	58.4	54.4	1.2	5	3E+04
	4.7	8.07	200	0.4	55.8	54.3	0.8	6	3E+04
	8.1	8.05	28	<DL	53.0	55.1	0.5	NA	NA
	15.0	8.28	35	<DL	53.7	56.5	0.9	NA	NA
MA70138 fracture water	0	7.71	4940	25.6	93.1	51.5	0.5	6	4E+04
	0.4	7.85	2370	5.0	77.7	52.5	1.3	8	5E+04
	0.8	7.90	1790	7.0	70.0	52.2	1.4	7	4E+04
	1.3	7.98	1410	9.2	65.3	51.1	1.0	8	5E+04
	2.3	7.99	1070	5.2	62.8	49.2	0.4	10	6E+04
	4.8	7.90	900	4.0	58.7	49.4	0.2	8	5E+04
	8.2	7.90	490	4.7	52.4	48.5	0.5	6	4E+04
	15.1	8.10	240	5.6	49.3	47.7	0.1	5	3E+04
MA70138 fracture water with air purging	0	7.71	4940	25.6	93.1	51.5	0.5	6	4E+04
	0.8	7.85	2630	6.9	79.6	50.5	1.0	8	5E+04
	1.3	7.85	2210	7.0	73.3	50.5	0.8	8	5E+04
	2.3	7.88	1400	3.8	64.7	50.9	0.7	7	4E+04
	4.8	8.12	830	2.6	58.9	49.2	0.2	9	5E+04
	8.2	8.12	280	1.2	53.0	50.6	0.2	6	4E+04
	15.1	ND	310	<DL	51.5	51.0	0.4	NA	NA

*ND – no data; <DL – below detection limit; NA – not available.

NIH-PA Author Manuscript
NIH-PA Author Manuscript
NIH-PA Author Manuscript

Table 5

Concentrations of arsenic, iron and other trace elements in the settled particles at the end of cubitainer experiments

	particle Fe weight ratio	particle As (mg/kg)	particle As/Fe (mmol/mol)	particle P (mg/kg)	particle S (mg/kg)	particle Mn (mg/kg)
MA70076 borehole water	28%	1140	3	730	930	1800
MA70076 fracture water	24%	1180	4	720	1300	1820
MA70076 borehole water - air	20%	780	3	760	1800	1130
MA70076 fracture water - air	19%	870	3	1540	2690	1460
MA70138 borehole water	35%	3020	6	1110	1010	3510
MA70138 fracture water	27%	2930	8	970	480	1560
MA70138 borehole water - air	19%	1910	7	1190	1830	1670
MA70138 fracture water - air	14%	1570	8	820	1750	770

* "-air" indicates air purged experiments.